National Development Plan 2007 - 2013

Environmental Protection Agency
An Ghníomhaireacht um Chaomhnú Comhshaoil

STRIVE
Report Series No.70

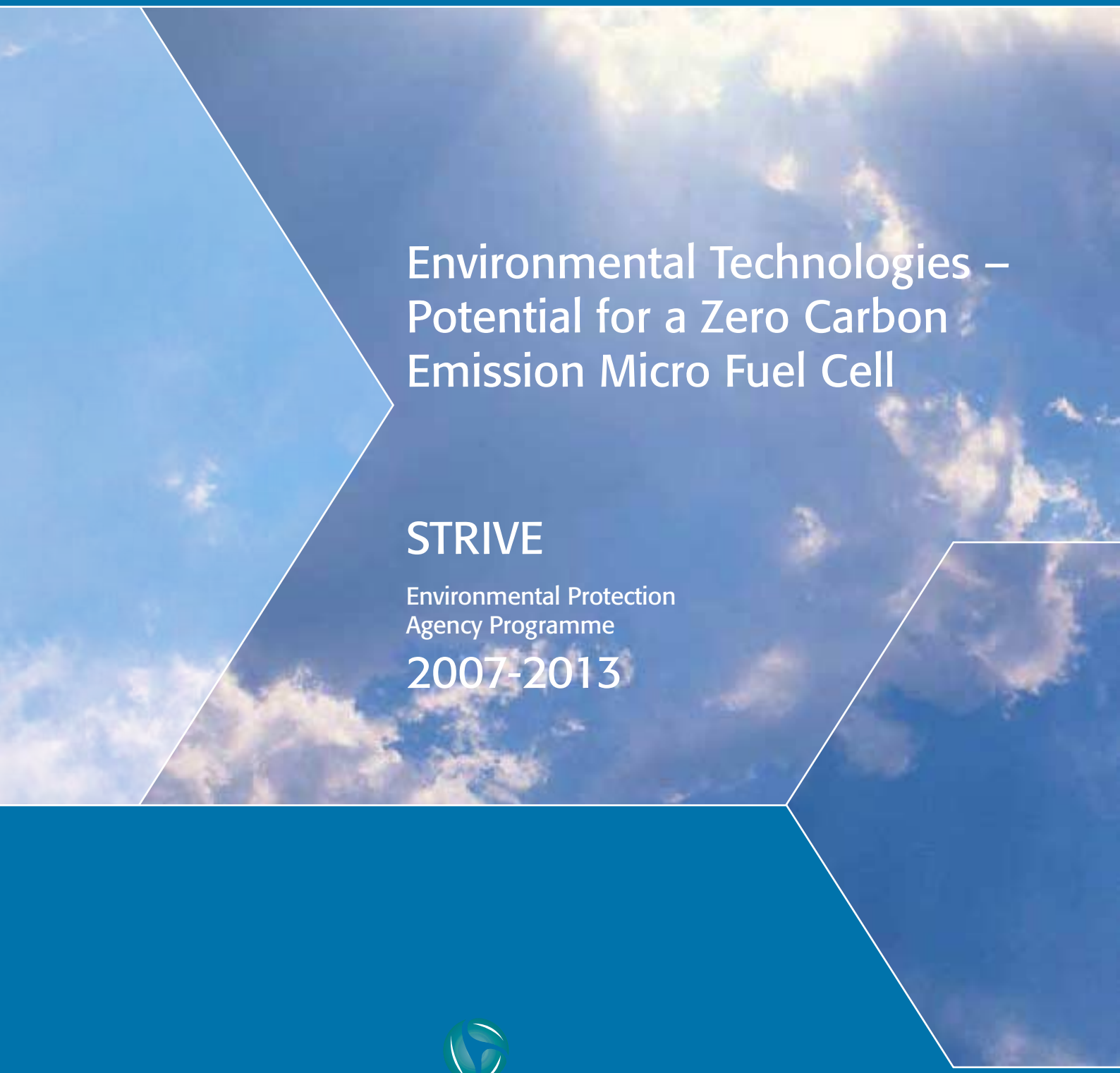

Environmental Technologies – Potential for a Zero Carbon Emission Micro Fuel Cell

STRIVE

Environmental Protection Agency Programme

2007-2013

SSTI

Comhshaol, Pobal agus Rialtas Áitiúil
Environment, Community and Local Government

Environmental Protection Agency

The Environmental Protection Agency (EPA) is a statutory body responsible for protecting the environment in Ireland. We regulate and police activities that might otherwise cause pollution. We ensure there is solid information on environmental trends so that necessary actions are taken. Our priorities are protecting the Irish environment and ensuring that development is sustainable.

The EPA is an independent public body established in July 1993 under the Environmental Protection Agency Act, 1992. Its sponsor in Government is the Department of the Environment, Community and Local Government.

OUR RESPONSIBILITIES

LICENSING

We license the following to ensure that their emissions do not endanger human health or harm the environment:

- waste facilities (e.g., landfills, incinerators, waste transfer stations);
- large scale industrial activities (e.g., pharmaceutical manufacturing, cement manufacturing, power plants);
- intensive agriculture;
- the contained use and controlled release of Genetically Modified Organisms (GMOs);
- large petrol storage facilities;
- waste water discharges.

NATIONAL ENVIRONMENTAL ENFORCEMENT

- Conducting over 2,000 audits and inspections of EPA licensed facilities every year.
- Overseeing local authorities' environmental protection responsibilities in the areas of - air, noise, waste, waste-water and water quality.
- Working with local authorities and the Gardaí to stamp out illegal waste activity by co-ordinating a national enforcement network, targeting offenders, conducting investigations and overseeing remediation.
- Prosecuting those who flout environmental law and damage the environment as a result of their actions.

MONITORING, ANALYSING AND REPORTING ON THE ENVIRONMENT

- Monitoring air quality and the quality of rivers, lakes, tidal waters and ground waters; measuring water levels and river flows.
- Independent reporting to inform decision making by national and local government.

REGULATING IRELAND'S GREENHOUSE GAS EMISSIONS

- Quantifying Ireland's emissions of greenhouse gases in the context of our Kyoto commitments.
- Implementing the Emissions Trading Directive, involving over 100 companies who are major generators of carbon dioxide in Ireland.

ENVIRONMENTAL RESEARCH AND DEVELOPMENT

- Co-ordinating research on environmental issues (including air and water quality, climate change, biodiversity, environmental technologies).

STRATEGIC ENVIRONMENTAL ASSESSMENT

- Assessing the impact of plans and programmes on the Irish environment (such as waste management and development plans).

ENVIRONMENTAL PLANNING, EDUCATION AND GUIDANCE

- Providing guidance to the public and to industry on various environmental topics (including licence applications, waste prevention and environmental regulations).
- Generating greater environmental awareness (through environmental television programmes and primary and secondary schools' resource packs).

PROACTIVE WASTE MANAGEMENT

- Promoting waste prevention and minimisation projects through the co-ordination of the National Waste Prevention Programme, including input into the implementation of Producer Responsibility Initiatives.
- Enforcing Regulations such as Waste Electrical and Electronic Equipment (WEEE) and Restriction of Hazardous Substances (RoHS) and substances that deplete the ozone layer.
- Developing a National Hazardous Waste Management Plan to prevent and manage hazardous waste.

MANAGEMENT AND STRUCTURE OF THE EPA

The organisation is managed by a full time Board, consisting of a Director General and four Directors.

The work of the EPA is carried out across four offices:

- Office of Climate, Licensing and Resource Use
- Office of Environmental Enforcement
- Office of Environmental Assessment
- Office of Communications and Corporate Services

The EPA is assisted by an Advisory Committee of twelve members who meet several times a year to discuss issues of concern and offer advice to the Board.

EPA STRIVE Programme 2007–2013

Environmental Technologies – Potential for a Zero Carbon Emission Micro Fuel Cell

Zero Carbon Emission Micro Fuel Cell Design

(2007-ET-FS-6-M5)

STRIVE Report

Prepared for the Environmental Protection Agency

by

Tyndall National Institute

Authors:

Lorraine Nagle and James Rohan

ENVIRONMENTAL PROTECTION AGENCY

An Ghníomhaireacht um Chaomhnú Comhshaoil
PO Box 3000, Johnstown Castle, Co.Wexford, Ireland

Telephone: +353 53 916 0600 Fax: +353 53 916 0699
LoCall: 1890 33 55 99
Email: info@epa.ie Website: www.epa.ie

ACKNOWLEDGEMENTS

This report is published as part of the Science, Technology, Research and Innovation for the Environment (STRIVE) Programme 2007–2013. The programme is financed by the Irish Government under the National Development Plan 2007–2013. It is administered on behalf of the Department of the Environment, Community and Local Government by the Environmental Protection Agency which has the statutory function of co-ordinating and promoting environmental research.

DISCLAIMER

Although every effort has been made to ensure the accuracy of the material contained in this publication, complete accuracy cannot be guaranteed. Neither the Environmental Protection Agency nor the author(s) accept any responsibility whatsoever for loss or damage occasioned or claimed to have been occasioned, in part or in full, as a consequence of any person acting, or refraining from acting, as a result of a matter contained in this publication. All or part of this publication may be reproduced without further permission, provided the source is acknowledged. The EPA STRIVE Programme addresses the need for research in Ireland to inform policymakers and other stakeholders on a range of questions in relation to environmental protection. These reports are intended as contributions to the necessary debate on the protection of the environment.

EPA STRIVE PROGRAMME 2007–2013

ISBN: 978-1-84095-395-4

Price: Free **Online version**

Details of Project Partners

Dr Lorraine Nagle
Tyndall National Institute
Lee Maltings
Dyke Parade
Cork
Ireland.
Tel.: +353 21 490 4266
Email: lorraine.nagle@tyndall.ie

Dr James Rohan
Tyndall National Institute
Lee Maltings
Dyke Parade
Cork
Ireland.
Tel.: +353 21 490 4224
Email: james.rohan@tyndall.ie

Table of Contents

Executive Summary

As the impact of the over-dependence on fossil fuels becomes more apparent on the gradual climate change and the deterioration of the environment, the search for clean, efficient and safer energy sources is becoming increasingly important. The impetus for this project came from the need to develop low-carbon or decarbonised energy sources. This entailed the design of a prototype direct borohydride fuel cell (DBFC) using a novel nanoporous gold (NPG) anode catalyst to realise the maximum output from a 'zero carbon emission' fuel – sodium borohydride. The advantages of a borohydride fuel cell include the high-energy density of borohydride coupled to the emission of carbon-free by-products. Borohydride is non-toxic, easy to store and transport and its by-products can be regenerated into borohydride. This study unveils nanoporous gold as a remarkably efficient anode catalyst for a DBFC.

This STRIVE project focused specifically on exploiting the properties of NPG – in particular, the large specific surface area combined with a high density of defect sites – to develop a DBFC anode catalyst with high catalytic activity for oxidation of BH_4^- and low activity for its competing hydrolysis. NPG electrodes were fabricated in a range of film and wire array formats by selectively dealloying silver from silver–gold alloys. Borohydride oxidation was studied by cyclic voltammetry at the NPG electrodes. The onset potential for the oxidation at a NPG wire array was found to shift to more negative potentials than that observed at a planar gold disc, and higher currents were realised. An onset potential of -1.07 voltage (V) vs standard calomel electrode (SCE) which is 0.207 V lower than that at a gold disc was recorded. The oxidation current for 20 mM borohydride in 2 M sodium hydroxide increased to 73.6 mA cm^{-2} from 3.17 mA cm^{-2} at a gold disc. A value of 7.85 electrons was determined for n out of a possible 8 for borohydride oxidation. These criteria point to a highly favourable and efficient catalyst for borohydride oxidation. In addition, facile and efficient oxidation of two other high-energy density fuels (ammonia borane and dimethylamine borane) at NPG that also do not emit carbon by-products was demonstrated. The results are consistent with an overall hypothesis that the central difference between NPG and bulk Au is caused by the increased density of step edges in NPG relative to bulk Au. This opens exciting new avenues for catalyst design.

Nanoporous gold presents an attractive alternative to gold nanoparticle-based catalysts for fuel cells in that it does not require a carbon support, thereby removing the stability issues associated with carbon-supported gold nanoparticle systems. NPG may be incorporated as a thin foil as a porous catalyst electrode as it is shapable and has high mechanical, thermal and chemical stability coupled with high catalytic activity. It has a dual functionality in that it can act as a current collector and as a catalyst, and it may also be integrated into nafion-based membrane electrode assemblies (MEAs) in conventional polymer electrolyte membrane (PEM) fuel cells. An advantage of incorporating NPG over platinum in fuel cells would be the useful enhancement in electrical conductivity that could be derived because of the lower electrical resistivity of gold. Nanoporous gold can provide a solution to the sintering problems that plague nanoparticle-based catalysts, and it also allows for the establishment of more intimate contact with an electrical substrate. The porous structure promotes mass transport of the reactant to the active sites and the release of gaseous by-products. The diffusion of an electroactive species to gold nanoparticles on a high-surface-area carbon support is limited by the low degree of porosity of the support.

A prototype miniature DBFC (1 cm^2 in size) was constructed using printed circuit board (PCB) plates with manganese dioxide as a cathode and NPG as an anode. The prototype miniature DBFC was tested for in terms of stability and output power with the view to unveiling a competitive, environmentally cleaner energy carrier. The cell was tested using borohydride at concentrations of 20 mM and 75 mM borohydride in 2 M sodium hydroxide. An open circuit potential (OCV) of 0.66 V was recorded. For 20 mM borohydride, a current density of 3.0 mA cm^{-2} was recorded at a voltage of 0.20 V and the maximum power density recorded was 0.63 mW cm^{-2}.

Identifying innovative energy solutions plays a vital role in responding to environmental-protection challenges and societal needs. Fuel cells can play a key part in delivering on the objectives of Ireland's 'smart green' economy through the generation of cleaner and more efficient power that places less stress on the environment due to a decrease in emissions related to energy production. The research findings reported here unveil a cleaner energy technology that can compete in national and international markets. The EPA envisages that its research programmes will continue to develop significant research expertise and be recognised as a leading activity supporting the smart green economy. The development and deployment of fuel cells as cleaner energy sources deserves support in EPA's future strategy.

1 Introduction

1.1 Objectives

The objectives of the research were to:

1 Design a novel porous gold anode catalyst for a direct borohydride fuel cell (DBFC);

2 Obtain electrochemical data on the efficiency of the novel catalyst;

3 Integrate the novel catalyst with ancillary components into a prototype DBFC;

4 Analyse DBFC in terms of fuel consumption, output energy, power density, released by-products and total cost;

5 Publish data in peer-reviewed journals and present at conferences and workshops to highlight the DBFC based on the novel nanoporous gold (NPG) anode as a competitive and environmentally cleaner energy carrier;

6 Support the development of decarbonised energy technologies in an effort to reduce carbon emissions.

1.2 Literature Review

1.2.1 Fuel Cell Technology

Fuel cells have been widely recognised as a promising energy technology because of their high-energy conversion efficiency and environmental friendliness (Jacobson et al., 2005; Steele and Heinzel, 2001). Key requirements of a fuel cell are that the fuel should be readily available, safe and easily transported, rapidly oxidised at a negative potential, and available to the fuel cell anode in a concentrated form with a large energy and power output/unit weight of fuel. Among the various categories of fuel cells, the proton exchange membrane fuel cell (PEMFC), using hydrogen as fuel, is the most advanced fuel cell today. However, the difficulties associated with the mobile storage of hydrogen remain a major obstacle to the commercialisation of PEMFC. As a result, research and development works are also carried out on fuel cell systems using alternative fuels, such as alcohols (especially methanol) and borohydride. In principle, these alternative fuels can be used either directly or indirectly. Direct electro-oxidation of a fuel in a fuel cell gives a more compact device because it does not have a separate fuel reformer. However, before this advantage can be exploited in a fuel-cell system, the challenge of finding an anode that can perform a specific and efficient direct oxidation of a fuel must be met.

1.2.2 Fuel Cells as Portable Power Sources

Various fuel cells are being developed as portable power sources to meet higher energy demands as well as to extend the operational hours of portable electronic devices. Rapid developments of portable electronic devices demand new power sources with higher energy density than currently used lithium-ion batteries to achieve longer operation hours and shorter recharging time. Liquid fuel cells such as direct methanol fuel cells (DMFCs) are attractive because of the higher energy density of the liquid fuel, their ease of integration with portable devices, the high-energy density of methanol and the ease of handling of liquid fuel. However, the widespread commercialisation of DMFCs is delayed due to their low power output owing to sluggish electrode kinetics and methanol crossover.

The current status of DMFC performance is still far from the requirements needed for commercialisation. The major obstacles encountered in the development of the DMFC are the low activity of methanol and its crossover to the cathode side. The toxicity of methanol is another major concern. Recent vigorous research on the direct borohydride fuel cell (DBFC) has raised the expectation for the realisation of the various benefits promised by this fuel cell system for portable applications greatly (Wee, 2006). Existing battery technologies do not appear to demonstrate the required rate of improvement to match the ever increasing power demands of portable electronic devices in the near future (Krishnan et al., 2008).

1.2.3 Direct Borohydride Fuel Cells

Alkaline borohydrides, especially sodium borohydride ($NaBH_4$) have many advantages when compared with other liquid fuel cells. Sodium borohydride has received

recent support as a fuel which is available as a solid or a 30% solution in concentrated sodium hydroxide. For example, $NaBH_4$ has higher volumetric (7314Wh l^{-1}) as well as gravimetric (7100Wh kg^{-1}) energy density than methanol (4800Wh l^{-1}, and 6000Whkg^{-1}, respectively). Though the energy density of the fuels will be less due to dilution – namely a $NaBH_4$ solution in DBFC and methanol solution in DMFC – the difference is worth noting. Apart from this, BH_4^- solutions are also less toxic, and borohydride is less flammable and less volatile than gasoline.

Borohydride is an attractive alternative fuel for use in fuel cells because of its high-energy density and the ease with which it can be stored and transported (Ponce de Leon et al., 2006; Amendola et al., 1999). The by-products from the cell are water and sodium borate (borax) which are environmentally safe and carbon neutral. Indeed, borax is a harmless constituent used in detergents and as a soap additive, and can be re-hydrogenated into borohydride by several different techniques that require nothing more than water and electricity or heat. Facile kinetics of the oxygen reduction reaction (ORR) under alkaline conditions could enable the use of non-precious electrocatalysts for the cathode in a DBFC. Direct borohydride fuel cells provide higher power output per mass than DMFCs and could be produced more cheaply than DMFCs (which need expensive platinum catalysts). The threat to Artic human populations posed by increased levels of platinum in Greenland ice resulting from the use of platinum in catalytic converters has been highlighted in the European Environment Agency (EEA) report on health and the environment (European Environment Agency, 2005). Because of these advantages, DBFC presents a cleaner energy technology that merits investigation in an effort to develop environmentally clean sustainable power sources. As Equations 1.1 and 1.2 show, DBFC decomposes and oxidises borohydride fuel directly:

Cathode: $2O_2 + 4H_2O + 8e^- \Rightarrow 8OH^-$ $E^0 = 0.4$ V (Eq. 1.1)

Anode: $NaBH_4 + 8OH^- \Rightarrow NaBO_2 + 6H_2O + 8e^-$ $E^0 = 1.24$ V (Eq. 1.2)

Total $E^0 = 1.64$ V

The equilibrium voltage compares favourably with DMFC and H_2/O_2 fuel cells that have equilibrium voltages of 1.21 V and 1.24 V, respectively. Borohydride is a promising fuel given its high theoretical specific energy (9296 Wh/kg), high specific capacity (5.67 Ah/g) and good anode performance. The DBFC target specification is 600–1000 Wh kg^{-1}, which is 5–6 times the energy density of silver-zinc or lithium-ion batteries.

The first DBFC system was proposed in the early 1960s when Indig and Snyder (1962) reported a practical demonstration of direct electricity generation from borohydride ions. Research on DBFC technology then stagnated until the late 1990s when Amendola et al. (1999) reported on the performance of a DBFC system that used an Au–Pt alloy electroplated on carbon cloth as the anode, while the cathode was a commercial gas-diffusion electrode and was separated from the anode by an anode electrolyte membrane. Following further impressive research efforts over the next five years the first demonstration of a DBFC system for laptop computers was presented in 2005 by the Materials and Energy Research Institute (MERIT). MERIT succeeded in increasing the DBFC system output from 10 to 400 W (Barrett, 2005). Darren Browning (DSTL, UK) outlined their programme on fuel cells for a variety of military applications, including propulsion systems for unmanned underwater vessels, unmanned aerial vehicles, sonobuoys and army equipment (Cameron, 2006).

There are three types of DBFC as determined by the choice of electrolyte. When potassium hydroxide solution or an anion-exchange membrane (AEM) is employed as the electrolyte, the cathode-to-anode transfer of OH^- ions functions as both the charge carrier and the ion migration. On the other hand, in DBFC systems with a cation-exchange membrane (CEM) electrolyte such as Nafion, Na^+ migrates from the anode to the cathode to carry the charges. While each system has its own advantages and disadvantages, the CEM electrolyte supports the most efficient DBFC system in terms of BH_4^- crossover and is therefore adopted in the DBFC system investigated in this review. The CEM–DBFC system uses the $NaBH_4$ solution directly, with the chamber fuel either being pre-filled into, or continuously supplied to, the chamber at each anode compartment.

One major obstacle in the development of DBFCs has been the hydrogen evolution at the anode, which causes low coulombic efficiency and safety problems. Careful

selection of the anode catalyst is crucial in minimising competing hydrolysis of BH_4^- (Eq. 1.3), resulting in heterogeneous, non-faradaic H_2 evolution:

$$BH_4^- + 2\ H_2O \Rightarrow BO_2^- + 4H_2 \qquad \text{(Eq. 1.3)}$$

In practice, the actual anodic reaction can be more realistically represented as Eq. 1.4:

$$BH_4^- + nOH^- \Rightarrow BO_2 + (n-2)\ H_2O + ne + (4-0.5\ n)\ H_2 \qquad \text{(Eq. 1.4)}$$

where n is the actual number of electrons released by BH_4^-. The evolution of H_2 not only decreases fuel utilisation but also lowers cell performance as ion movement in the anolyte is hindered by H_2 bubbles. Attaining a high n value by suppressing hydrolysis and accelerating oxidation is key to optimising DBFC coulombic efficiency and minimising safety issues from H_2 formation. Attempts to prevent hydrogen evolution during the oxidation of borohydride on a fuel cell anode have always resulted in a shift of the anode potential to values more positive than the reversible hydrogen electrode (RHE) potential, thus losing the advantages of DBFC in comparison to conventional hydrogen fuel cells. Several studies have been undertaken to identify the most efficient anode catalyst for BH_4^- oxidation. Platinum supported on conductive titanium oxides has been found to catalyse the 8-electron oxidation of borohydride without hydrogen evolution in a potential range more negative than RHE, which is desirable in order to have a DBFC that is practically applicable (Wang and Chen, 2008).

The mechanism of the direct 8-electron oxidation process is discussed on the basis of a synergistic effect at the surface of Pt/Ti2O catalyst. In order to realise a practical DBFC, two requirements must be met simultaneously. Firstly, the anode must work at potentials more negative than RHE; secondly, there must be no hydrogen evolution at the anode. However, these two requirements are an apparent paradox. All the presently known highly active catalysts for borohydride oxidation, such as Pt, Ni, and hydrogen storage alloys, are also highly active toward the hydrogen evolution reactions due to the mechanistic similarities of the reactions. Therefore, it seems impossible to fulfil the two basic requirements at the same time. Whenever hydrogen evolution occurs, it consumes some of the electrons produced by borohydride oxidation, and the apparent number of electrons of borohydride oxidation (***n***app), defined as the number of electrons generated by each borohydride anion to the external circuit, will be reduced to values more or less below 8. Some researchers were able to prevent hydrogen evolution during 8 e-oxidation of borohydride, but only at potentials more positive than the RHE, leading to a significant loss in cell voltage.

The direct oxidation of sodium borohydride at silver and gold electrocatalysts, either in bulk polycrystalline form or nanodispersed over high-area carbon blacks in a concentrated sodium hydroxide medium was studied by cyclic and linear voltammetry, chronoamperometry and chronopotentiometry (Chatenet et al., 2006). Gold and silver yield rather a complete utilisation of the reducer: around 7.5 electrons are delivered on these materials, versus 4 at the most for platinum as a result of the BH_4^- non-negligible hydrolysis taking place on this latter material. The kinetic parameters for the direct oxidation are better for gold than for silver. A strong influence of the ratio of sodium hydroxide versus sodium borohydride is found. Whereas the theoretical stoichiometry does forecast that 8 hydroxide ions are needed for each borohydride ion, the current project's experimental results prove that a larger excess hydroxide ion is necessary in quasi-steady state conditions. When the above-mentioned ratio is unity (1 M NaOH and 1 M $NaBH_4$), the tetrahydroborate ions' direct oxidation is limited by the hydroxide concentration, and their hydrolysis is no longer negligible. The hydrolysis products are probably BH_3OH^- ions, for which gold displays a rather good oxidation activity. Additionally, silver, which is a weak BH_4^- oxidation electrocatalyst, exhibits the best activity of all the studied materials towards the BH_3OH^- direct oxidation. Finally, carbon-supported gold nanoparticles seem promising as an anode material. It was found that BH_4^- oxidation was more efficient at carbon-supported gold nanoparticles than at bulk polycrystalline gold. The kinetics in terms of exchange current density were better for carbon-supported gold nanoparticles, while the half-wave potential and the onset of oxidation were lower.

Liu and Suda (2008) showed that DBFC anode performances including current efficiency were strongly dependent on electrode material as well as borohydride concentrations. Electrocatalysts including Pt, Pd, Au, Ag, Ni, Os and some hydrogen storage alloys have been tested as anode materials for DBFC.

Electrochemical oxidation of borohydride ions on an Au electrode proceeds mainly through the direct oxidation of BH_4^-, which showed the oxidation wave at around −0.4 V versus NHE, a potential much more positive than the theoretical potential. Therefore, the direct oxidation of borohydride ions on Au electrodes demonstrated high current efficiency but low voltage efficiency. On the other hand, anodic oxidation of borohydride on Ni, Pt, Pd takes place predominantly through the oxidation of hydrolysis intermediates such as BH_3OH^- or atomic hydrogen. They showed oxidation waves at potentials more negative than that of BH_4^-. Therefore, these electrodes usually show good power performance but reduced current efficiencies. In both cases, there are trade-offs between voltage and current efficiency, which is not desirable in fuel-cell development. It is very challenging to develop anode catalysts with both high voltage and current efficiency. Liu and Suda (2008) reported recent progress in the development of a micro-DBFC aiming for portable applications. The single-cell performance including power density and current efficiency was improved significantly by using composite anode materials and a nafion ionomer as the binder. Based on the improvements on single cell, planer multi-cell modules were constructed to show the feasibility of DBFCs as practical power sources. Good performance exhibited by these DBFC power units shows promise for their potential in practical applications.

1.2.4 Nanoporous Gold

Nanoporous gold (NPG) is formed using dealloying, the chemical etching process, which involves selective metal dissolution. This has an ancient history: Incan civilisation dealloyed Cu from the surface of Cu-Au alloys to create an illusion of a pure gold artefact known as 'depletion gilding'. In the 1970s Forty (1979) and later Pickering (1983) showed that depletion gilding of a less-noble metal from Au alloys results in an open, continuous nanoporous structure composed of Au. As the Ag atoms in an Au/Ag alloy are dissolved in acid, the remaining gold atoms gather together in clusters that create a rough surface, which causes gold to evolve into a porous material. Dealloyed gold atoms act like water droplets condensed on a pane of glass – the gold atoms condense into little clumps that grow into the backbone of a porous structure. The sponge-like 3D structure is a system of interconnecting pores/tunnels in a skeleton of filaments of the metal. The filament size can range from 5–50 nm and surface areas as high as 20 m^2g^{-1} with a porosity of 70% or higher are possible. Nanoporous gold is mechanically far stronger than is supposed on the basis of a scaling law, presumably because the ligament size in the nm range causes dislocation starvation. Biener et al. (2006) indicated that NPG brings together two seemingly conflicting properties – high strength and high porosity. They characterised the size-dependent mechanical properties of NPG using a combination of nanoindentation, column microcompression, and molecular dynamics simulations. Structurally, these materials bear a resemblance to naturally occurring zeolites (filament size 1–2 nm and surface areas 100 m^2g^{-1}) (Sieradzki and Karma, 2001). NPG is a useful but relatively unstudied form of gold that likely contains an intrinsically high-step density. Because NPG may be described as an interconnected, bicontinuous ligament network containing regions of both negative and positive curvature, a high-step density is topologically required. This characteristic makes NPG attractive for catalysis studies; it is made even more attractive because it can be easily formed into thin, high-conductivity foils that are adapted easily to electrocatalytic measurements. Recent interest in electrolytic de-alloying has been motivated by the realisation that nanoporous metals exhibit interesting properties (including a large specific surface area and oriented geometry) and the prospect of applying these materials as catalysts, sensors, coatings for medical devices, microreactors, actuators, microelectrodes, heat exchangers, filtration membranes, devices or precursors for making nanocrystalline gold. Generally, however, it is important to note that the pace of discovery of the number of reactions for which NPG by itself is a good catalyst is increasing rapidly, and many different systems in which NPG may be the superior catalyst remain to be examined.

Most likely, this useful but relatively unstudied, form of Au contains an intrinsically high-step density that makes it attractive for catalysis studies. In terms of catalytic applications, NPG has at least two advantages over other catalysts or Au nanoparticles.

Firstly, NPG remains active at low temperatures (room temperature or even lower), unlike Pt or Pd catalysts. Research has suggested that gold nanoparticle-based catalysts can display low temperature activity and selectivity under a range of conditions relevant to automotive pollution control (Pattricka et al., 2004).

Platinum group metals (PGMs) are currently used for both anode and cathode catalysts in most commercial proton exchange membrane (PEM) fuel cells. The tendency for poisoning of platinum by CO contaminant in the hydrogen feedstock gas remains a major technical hurdle. Gold was shown to have particularly good catalytic performance for the oxidation of carbon monoxide. However, compared to research focused on the use of PGMs for automotive pollution control, the science of gold catalysis is still in its infancy. Stable low-temperature CO oxidation over unsupported NPG was shown by Tian and Xu (2007). A significant CO conversion rate at -30 ° C was sustained for longer times than that recorded at room temperature. The room temperature deactivation originated from an increase in ligament size, which resulted in pore clogging and a decrease in active surface area. Low temperature CO oxidation over unsupported NPG in a foam-type structure was shown by Zielasek et al. (2006): NPG was shown to exhibit high CO oxidation activity. However, the catalytic reactions occur only at the surfaces of NPG foam.

Secondly, NPG exhibits good thermal stability and resistance to oxidation and thus can overcome the aggregation or sintering limitations that Au nanoparticles encounter at elevated temperatures or in an oxidative environment (Choudhary and Goodman, 2005). It was demonstrated by Zeis (2008) that NPG is an effective catalyst for the reduction of hydrogen peroxide to water. The reaction efficiency is sufficiently high to allow the use of the material as a cathode for oxygen reduction in hydrogen PEM fuel cells, although the overall efficiency in this context is still far less than that of Pt. Their results are consistent with the overall hypothesis that the central difference between NPG and bulk Au is caused by the increased density of step edges in NPG relative to bulk Au. In summary, using nanoporous gold electrodes for fuel cell electrodes opens exciting new avenues for catalyst design.

2 Methods

2.1 Materials Used

Sodium borohydride (minimum purity 98%), sodium carbonate (minimum purity 99%) and sodium hydroxide, NaOH (minimum purity 99%) were purchased from Sigma Aldrich and used as received. Potassium silver cyanide $KAg(CN)_2$ (minimum purity 99%) and potassium gold cyanide $KAu(CN)_2$ (minimum purity 99%) were purchased from Johnson Matthey and used as received. Anodisc alumina circular membranes (Anodisc® 25) 2.5 cm in diameter, 60 μ thick, 200 nm pore size and 10^9 pore openings per cm^2 of membrane were supplied by Whatman™. These show compatibility with a wide range of solvents and acids and can be dissolved in sodium hydroxide and ammonium hydroxide solutions. The maximum temperature at which they are stable is 400 °C. Deionised water of resistivity 18 MΩ cm was used to prepare all solutions. The working electrode was a 5 mm Au disc (Princeton Applied Research) supplied by Advanced Measurement Technology, UK. These were polished with 0.5 μm alumina powder obtained from Struers on a Buehler polishing cloth for 2 minutes and rinsed in deionised water. A 1 mm diameter Au of 50 mm length and standard calomel electrode were used as counter and reference electrode, respectively.

2.2 Electrochemical Measurements

Cyclic voltammograms (CVs) were recorded with respect to a standard calomel electrode (SCE). The potential of the working electrode was controlled using a CH Instruments potentiostat model 660B with picoamp booster. All solutions were purged with nitrogen for 20 minutes prior to experiments in order to remove oxygen, and the experiments were performed at room temperature.

2.3 Electron Microscopy Characterisation

Transmission electron micrograph TEM images were recorded using JEOL 2000FX at an accelerating voltage of 200 kV. Scanning electron micrograph SEM images were recorded using Nova Nanosem 630 at an accelerating voltage of 15 kV.

2.4 X-ray Diffraction Analysis

X-ray diffraction (XRD) images were recorded with an X'Pert PRO MRD made by PANalitical equipped with a PW3050/65 X'Pert PRO high-resolution goniometer. Scans were recorded with PW3011/20 with slit of 1/4deg. The monochromator used was 4xGe220 Sym. (mirror) and the wavelength of operation was 1.5418 Å.

3 Results

3.1 Fabrication of Nanoporous Gold

NPG was fabricated on a planar Au film and in a 3D-wire array format. It was shown by Searson et al. (2003) that $Au_{0.18}Ag_{0.82}$ alloy can be deposited from a solution of 100 mM $KAg(CN)_2$ and 20 mM $KAu(CN)_2$ in 250 mM Na_2CO_3, pH 13, at a constant potential of -1.2 V, and they determined the alloy composition by X-ray Photon Spectroscopy (XPS) analysis. A film of $Au_{0.18}Ag_{0.82}$ was deposited herein on a 200 nm Au film on a pyrex wafer for 5000 seconds according to this method. It was demonstrated that the morphology and porous structure of NPG depends on the composition of the $A_{gx}A_{uy}$ alloy for the range $0.18 \leq x \geq 0.32$ (Searson et al., 2003). The alloy composition $Au_{0.18}Ag_{0.82}$ gives the highest surface area NPG (6.9 m^2 g^{-1}) when subsequently dealloyed in nitric acid and the shortest ligament size of 20–30 nm. The deposition of the alloy is shown in the CV in Fig. 3.1. Current density is plotted on the vertical axis against potential on the horizontal axis

The CV of the resulting alloy in 1 M NaOH shown in Fig. 3.2 indicated the presence of Au and Ag from the metal oxide reduction peaks seen at -0.1 V and 0.4 V, respectively.

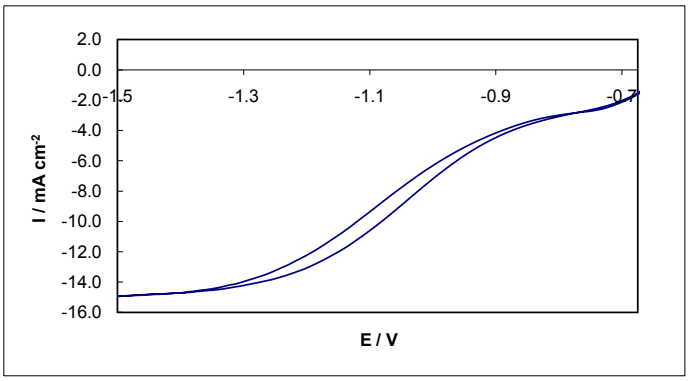

Figure 3.1. Deposition of silver-gold alloy on a gold rotating disc electrode (RDE) in a solution of 100 mM $KAg(CN)_2$ and 20 mM $KAu(CN)_2$ in 250 mM Na_2CO_3 at pH 13.

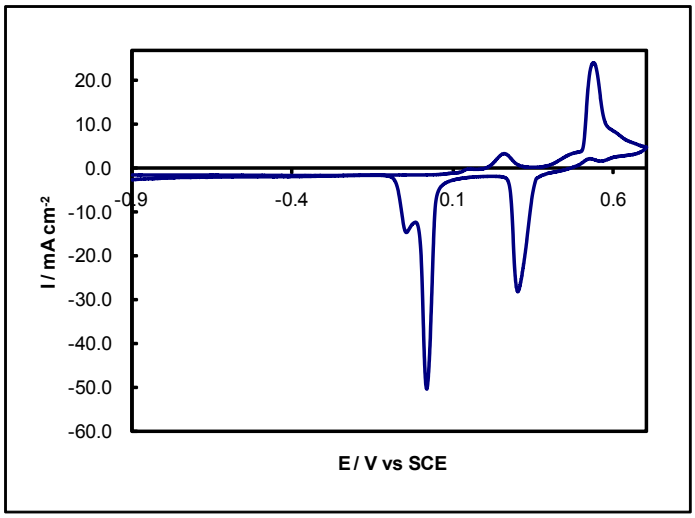

Figure 3.2. Cyclic voltammetric (CV) response for silver-gold alloy deposited on gold rotating disc electrode (RDE) in 1 M NaOH.

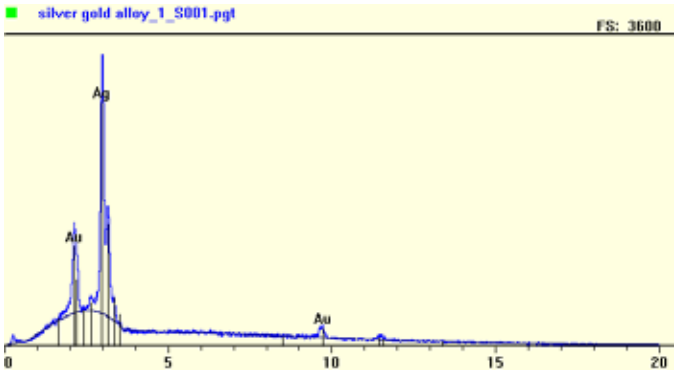

Element	Wt %	Atomic %	ChiSquared	Gross (cps)	BKG (cps)	Net (cps)
Ag	74.40	84.15	4.33	246.1	51.2	197.1
Au	25.60	15.85	8.67	124.8	47.3	45.5
Total	100.00	100.00	1.21			

Figure 3.3. Elemental detection analysis (EDX) spectrum for silver-gold alloy on gold wafer.

Elemental detection analysis (EDX) revealed that an alloy composition of $Au_{0.18}Ag_{0.82}$ was formed. The EDX spectrum is shown in Fig. 3.3.

The silver component was etched from the alloy by immersing it in 30% nitric acid for 60 minutes to obtain a high-surface area form of Au, NPG. The CV response recorded for NPG in 1 M NaOH from −0.95 to 0.70 V vs SCE at 10 mV s^{-1} (not shown here) indicated the presence of Au from the metal oxide reduction peaks seen at -0.10 V and the absence of Ag from the disappearance of the oxide reduction peak at 0.40 V associated with silver that was observed in the alloy. The thickness of NPG was measured as 2 micron using SEM. The NPG film was delaminated from the underlying Au film and sandwiched in a holey Cu folding TEM grid in order to obtain the TEM image shown in Figs 3.4-3.5. The pore and ligament size are 15 nm and 30 nm, respectively. The pore size of 15 nm can be seen in Fig. 3.5. The TEM images shown were recorded by sandwiching the NPG films in holey copper folding grids.

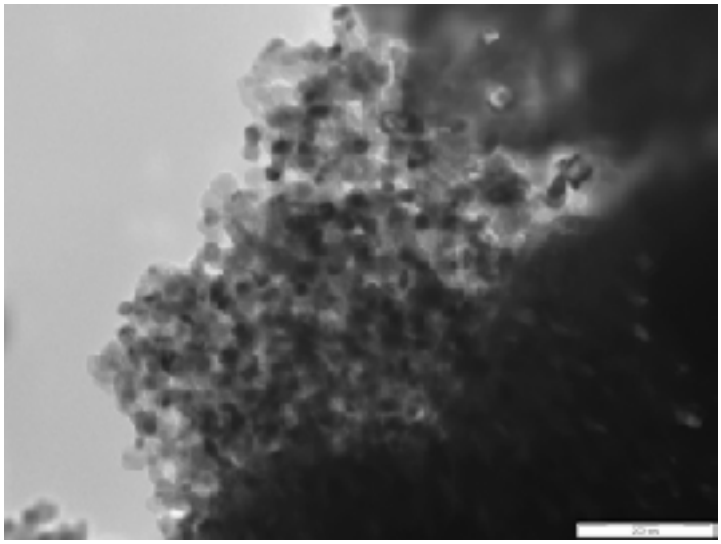

Figure 3.4. Transmission electron micrograph (TEM) image of nanoporous gold (NPG) film.

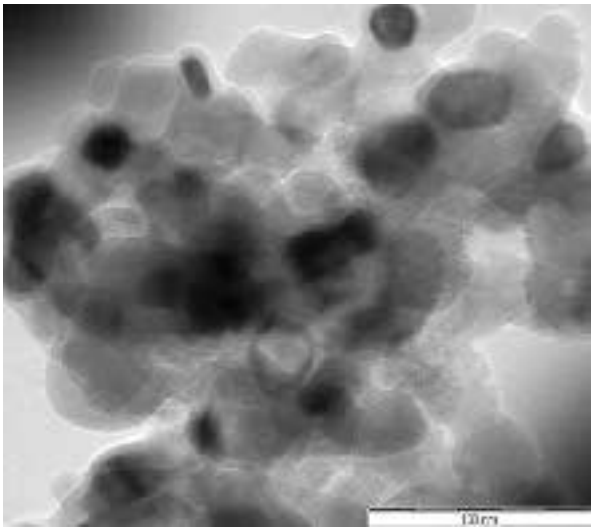

Figure 3.5. Transmission electron micrograph (TEM) image of nanoporous gold (NPG) film.

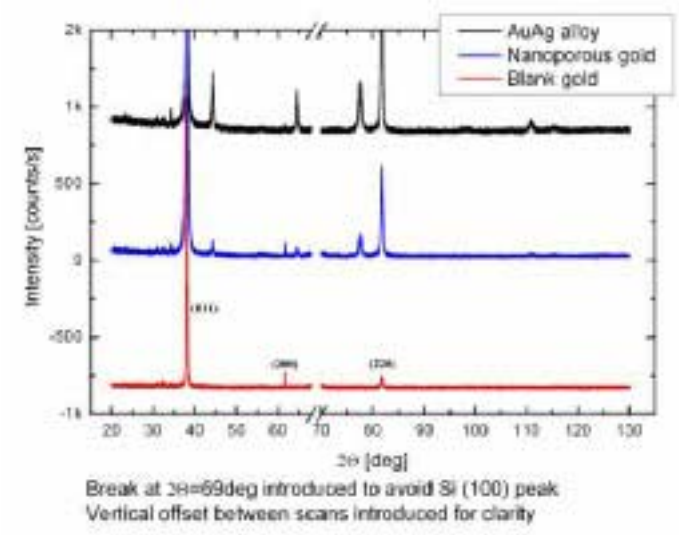

Fig. 3.6. X-ray diffraction (XRD) of nanoporous gold (NPG) film, silver-gold alloy and planar gold film (blank).

X-ray diffraction analysis of the alloy and NPG films were performed and compared with that of a clean Au film, as shown in Fig. 3.6. The presence of 111, 200 and 220 peaks was identified.

3.2 Fabrication of Nanoporous Gold in Wire-array Format

The fabrication of NPG in a 3D-wire array format was achieved by dealloying $Au_{0.18}Ag_{0.82}$ nanowires in nitric acid that were deposited in Anodisc alumina membranes with 200 nm pore size at a constant potential of -1.2 V from a solution of 100 mM $KAg(CN)_2$ and 20 mM $KAu(CN)_2$ in 250 mM Na_2CO_3, pH 13. The alumina membrane had a conducting backing layer of 350 nm Au which was e-beam evaporated. The alumina was dissolved by soaking it in 0.5 M NaOH for 2 hours to release the NPG wires. A schematic outline for the fabrication of a free-standing NPG catalyst array is illustrated in Fig. 3.7.

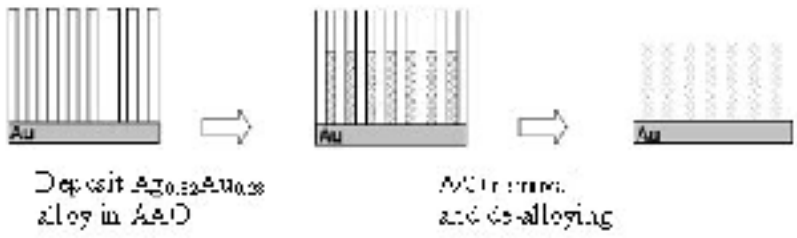

Fig 3.7. Route to fabrication of free-standing array of nanoporous gold wires.

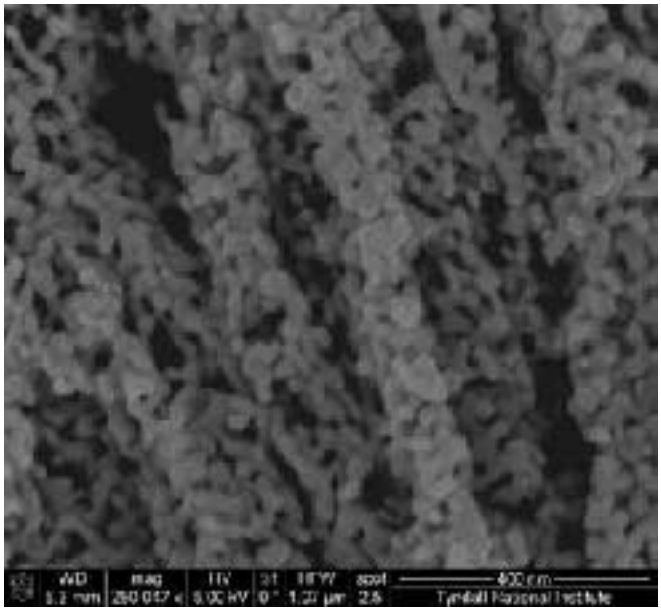

Figure 3.8. Scanning electron micrograph (SEM) image of nanoporous gold (NPG) wire array on Au.

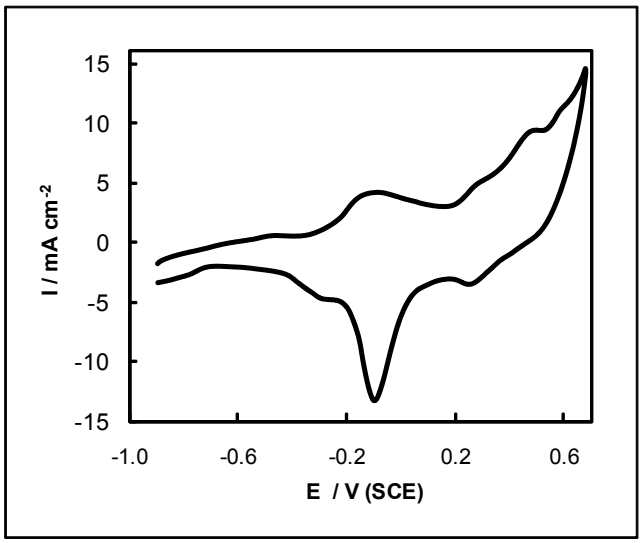

Figure 3.9. Cyclic voltammogram (CV) for nanoporous gold (NPG) wire array on a planar Au film in 1.0 mol dm^{-3} NaOH at 10 mV s^{-1}.

The SEM image shown in Fig. 3.8 was recorded for the resulting NPG wires. The fingerprint CV for the NPG wire array is shown in Fig. 3.9.

The oxidation of 20 mM borohydride at the NPG wire array electrode is shown in Fig. 3.10, where the maximum oxidation current is 73.6 mA cm^{-2}.

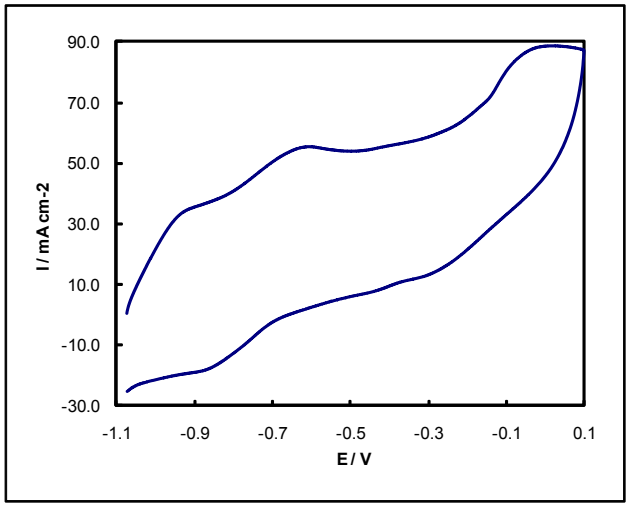

Figure 3.10. Cyclic voltammogram (CV) for NPG wire array on a planar Au film in 1.0 mol dm^{-3} NaOH with 20 mM borohydride recorded at 10 mV s^{-1}.

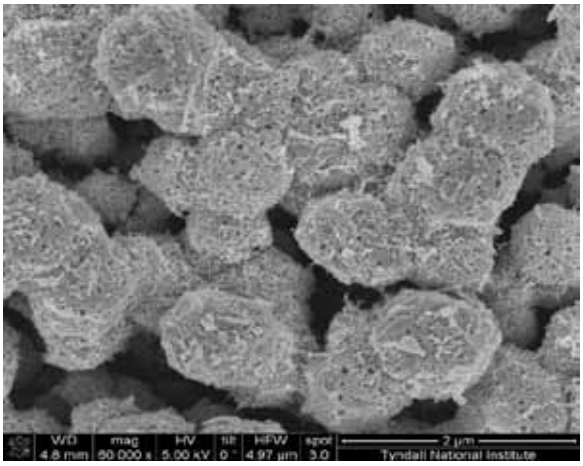

Figure 3.11. Scanning electron micrograph (SEM) image of nanoporous gold (NPG)-coated Au wire array on Au.

It was attempted to add structural rigidity to the NPG wire array by depositing (a) an NPG coating on a Au wire array and (b) NPG wires onto the ends of a Au wire array, as outlined below. This invariably leads to an increase in the amount of Au used in the electrode fabrication, however.

3.3 Fabrication of Nanoporous Gold-coated 3D Wire Array

A 3D Au wire array was deposited in Anodisc alumina membranes with a 350 nm Au conducting backing layer from a commercial Puramet bath. The Au wires were deposited to a length of 1 micron and 200 nm in diameter. The alumina was dissolved by soaking it in 0.5 M NaOH for 2 hours to release the Au wires. The Au wire array was then coated with NPG to a thickness of 20 nm. This was achieved by dealloying Ag_xAu_y nanowires that were deposited on the surface of the Au wires using the conditions given above for the fabrication of NPG on a planar Au film. The SEM image shown in Fig. 3.11 was recorded for the resulting NPG-coated Au wires. The fingerprint CV for the NPG wire array is shown in Fig. 3.12.

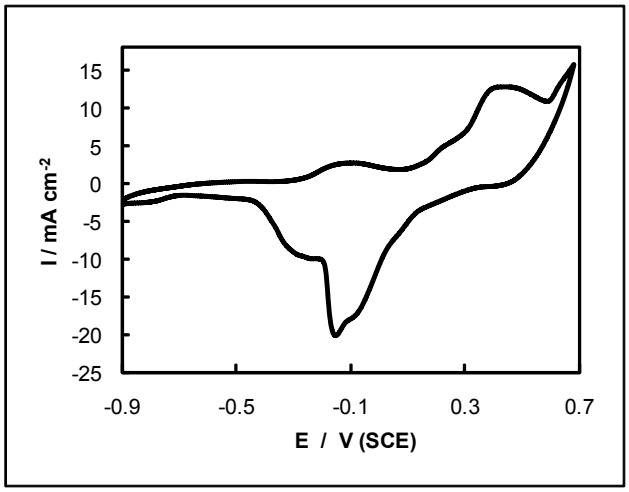

Figure 3.12. Cyclic voltammogram (CV) for nanoporous gold (NPG)-coated Au wire array on a planar Au film in 1.0 mol dm^{-3} NaOH recorded at 10 mV s^{-1}.

3.4 Fabrication of Segmented Nanoporous Gold-Au Wire Array

A 3D Au wire array was deposited in Anodisc alumina membranes with a 350 nm Au conducting backing layer from a commercial Puramet bath. The Au wires were deposited to a length of 3 micron and 200 nm in diameter.

The fabrication of NPG onto the Au wires was achieved by dealloying Ag_xAu_y wires that were then deposited on the Au wires in the Anodisc alumina membranes using the conditions given above for the fabrication of NPG on a planar Au film. The alumina was dissolved by soaking it in 0.5 M NaOH for 2 hours to release the segmented Au-NPG wires. The SEM image shown in Fig. 3.13 was recorded for the resulting segmented NPG-Au 3D wire array. The fingerprint CV for the NPG wire array is shown in Fig. 3.14.

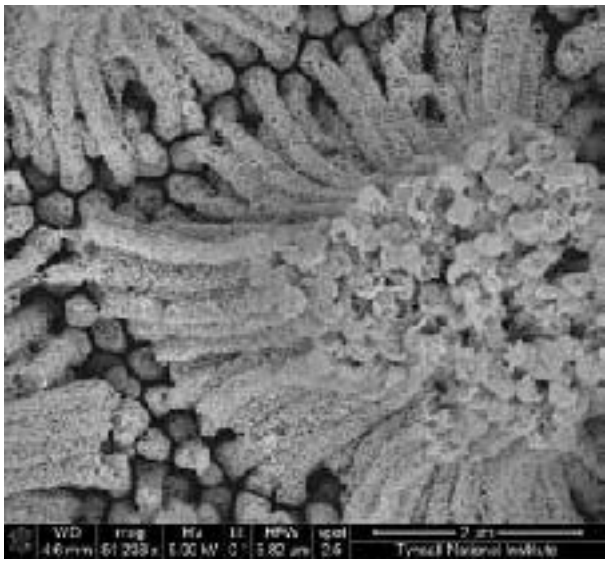

Figure 3.13. Scanning electron micrograph (SEM) image of segmented nanoporous gold-Au nanowire array on Au.

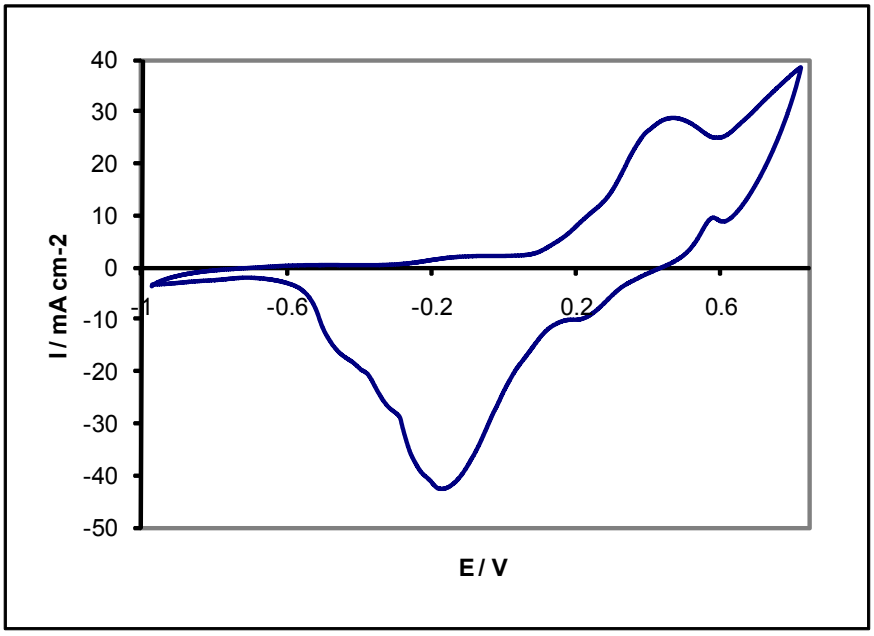

Figure 3.14. Cyclic voltammogram (CV) for segmented nanoporous gold-Au wire array on a planar Au film in 1.0 mol dm^{-3} NaOH recorded at 10 mV s^{-1}.

3.5 Cyclic Voltammetry Study of Borohydride Oxidation at Gold

Cyclic voltammograms (CVs) for an Au disc, NPG on the Au disc, NPG-Au segmented wire array and NPG wire array in 1 M NaOH are shown in Fig. 3.15. They clearly illustrate the influence of the increased surface area of the electrodes.

The oxidation response for 0.02 mol dm^{-3} $NaBH_4$ in 1 M NaOH at a**n** Au disc and NPG-coated Au disc under static conditions is shown in Fig. 3.15. The onset of oxidation at the Au disc is -0.80V and oxidation is sustained at the gold surface until 0.05 V when gold oxides that are inactive for BH_4^- oxidation form. In the subsequent reverse sweep, the oxidation recommences at 0.10 V upon gold oxide reduction. The onset of BH_4^- oxidation at the NPG-coated Au disc has shifted to -0.97 V. The peak a1 at -0.49 V has been reported previously in the literature and was assigned to the oxidation of a species in solution by Chatenet et al. (2009). This was attributed to a combination of hydrogen oxidation and the low potential oxidation of BH_4^-. The broad oxidation wave from -0.40 to 0.25 V in Fig. 3.16 may be attributed to the high-potential oxidation of BH_4^- and was shown to correspond to the oxidation of adsorbed BH_4^- species by Finkelstein et al. (2009).

The oxidation of BH_4^- is sustained into the region of gold oxide formation, indicating higher activity for the reaction than at the clean Au disc over this potential region. The BH_4^- oxidation current at the plateau centered at 0.0 V has increased from 3.17 at the Au disc to 38 mA cm^{-2} at the Au disc with NPG deposit.

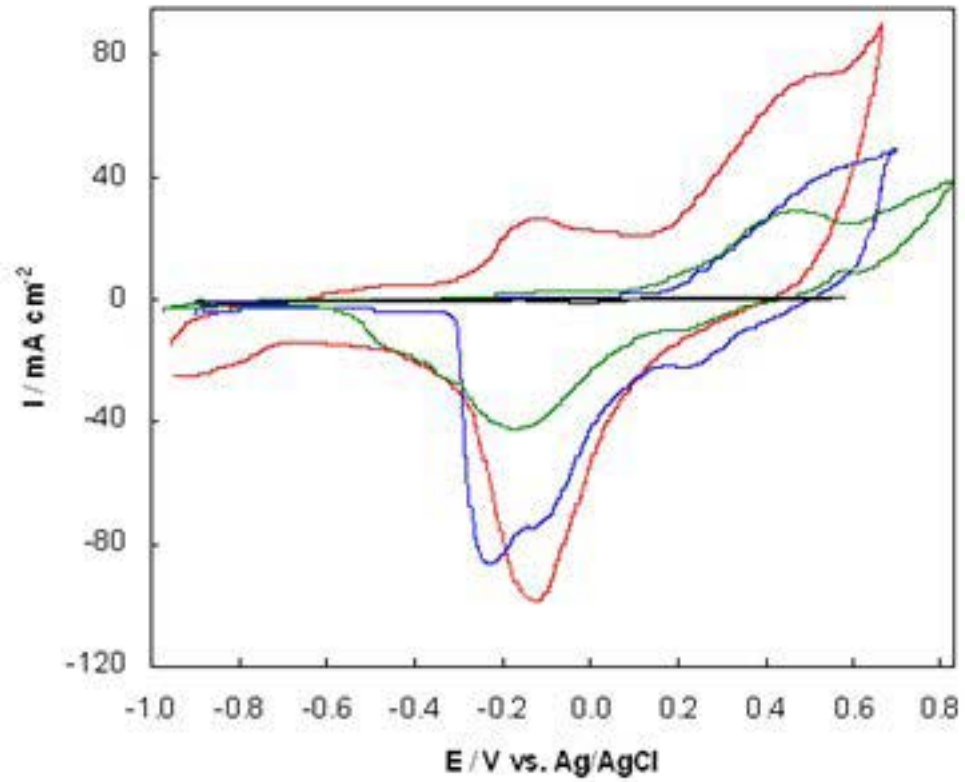

Figure 3.15. Cyclic voltammetric (CV) response for Au disc (black; I×20), nanoporous gold (NPG)-coated Au disc (blue), NPG-Au segmented wire array (green) and NPG wire array (red) electrodes in 1.0 mol dm-3 NaOH recorded at 10 mV s-1.

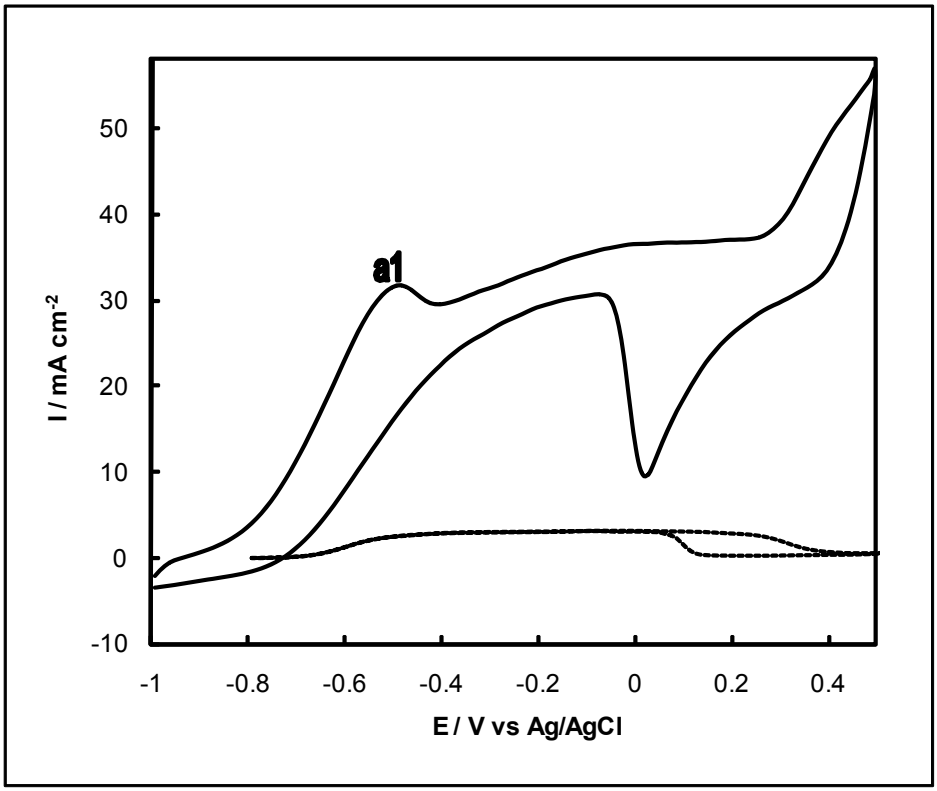

Figure 3.16. Cyclic voltammetric (CV) response for Au disc (- -) and nanoporous gold (NPG)-coated Au disc (-) in 1.0 mol dm^{-3} NaOH containing 0.02 mol dm^{-3} $NaBH_4$ under static conditions at 10 mV s^{-1}.

3.6 Determination of the Coulomb Number n for Borohydride Oxidation

The influence of the scan rate on the oxidation response for borohydride was studied at the NPG-coated Au disc. The positive shift of the peak potential for a1, $E_{p\ a1}$, with an increasing scan rate as shown in Fig. 3.17 is indicative of a sluggish reaction. The a1, peak current, $I_{p\ a1}$ increases linearly with the square root of scan rate as shown in Fig. 3.18: this suggests that a1 can be attributed to the oxidation of a species in solution and there is no interference from adsorption.

Using the Randles-Sevcik (Eqns 3.1 and 3.2) (Delahay, 1954) the number of electrons, n, associated with a1 was calculated as 4.26:

$$Ip = 2.99\times10^{5}\alpha^{1/2}n^{3/2}CD^{1/2}v^{1/2} \qquad \text{(Eq. 3.1)}$$

$$n\alpha = \frac{1.857RT}{\left(F(Ep - Ep_{0.5})\right)} \qquad \text{(Eq. 3.2)}$$

The n value obtained indicates the direct oxidation of BH_4^- is incomplete at -0.49 V and that its oxidation product is oxidised at more positive potentials. The influence of rotation rate on the oxidation response $NaBH_4$ was studied at the NPG-coated Au disc, as is shown in Fig. 3.19.

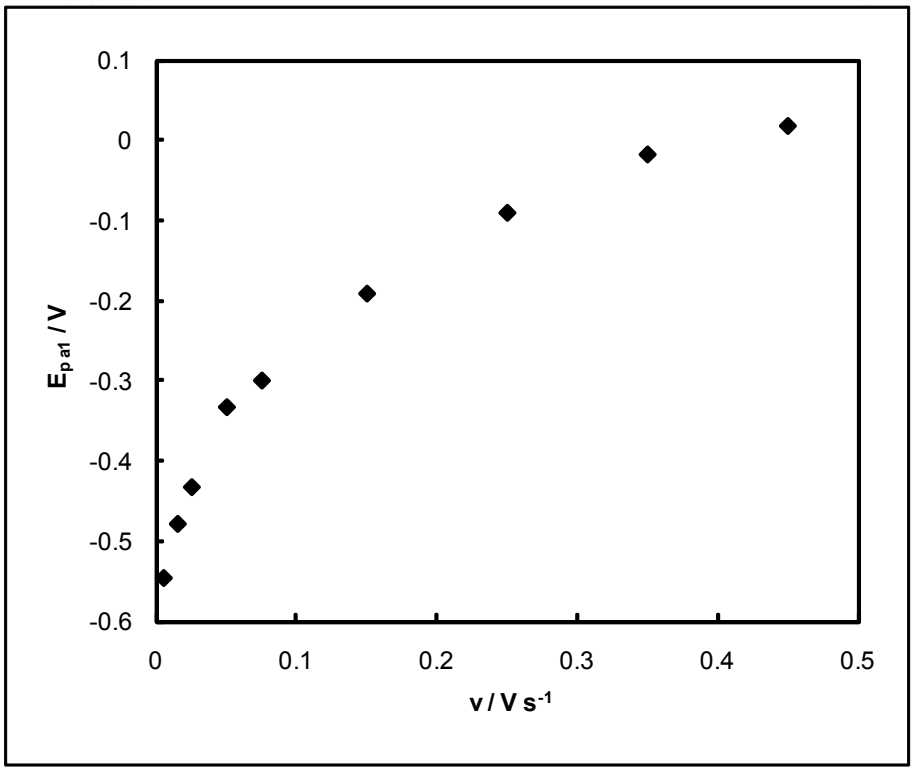

Figure 3.17. Peak potential for a1 at NPG-coated Au disc in 1.0 mol dm^{-3} NaOH containing 0.02 mol dm^{-3} $NaBH_4$ as a function of scan rate.

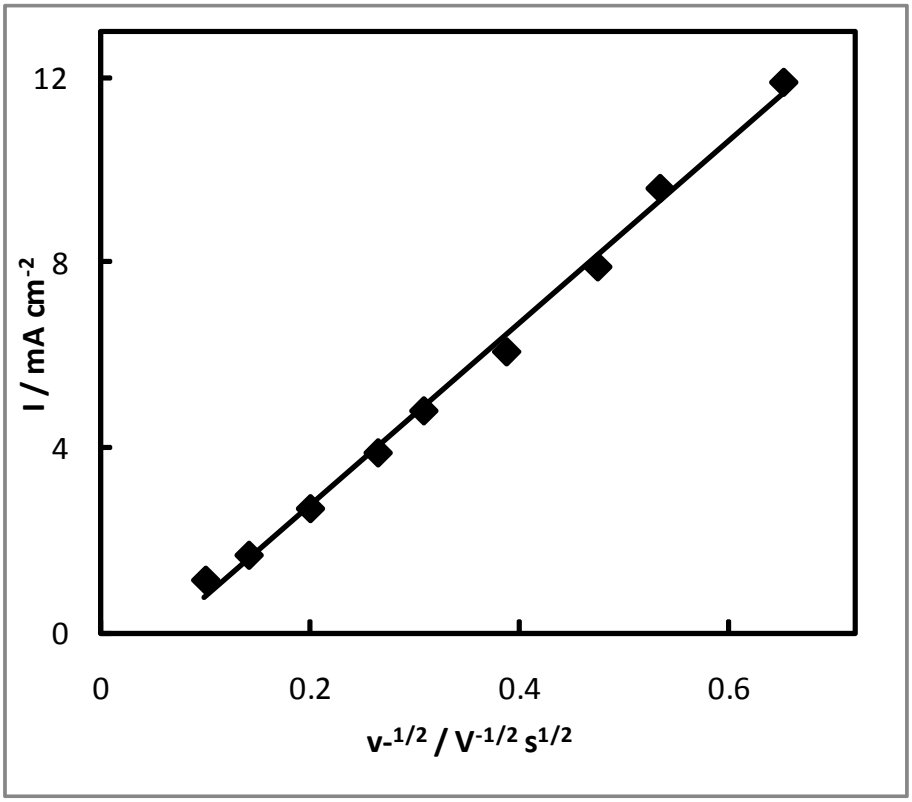

Figure 3.18. Peak current for a1 at nanoporous gold (NPG)-coated Au disc in 1.0 mol dm^{-3} NaOH containing 0.02 mol dm^{-3} $NaBH_4$ as a function of the square root of scan rate.

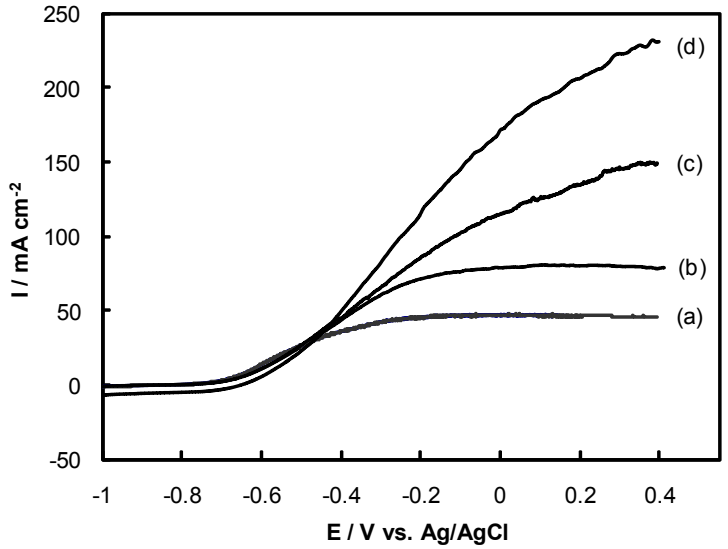

Figure 3.19. Linear sweep voltammetric response for NPG-coated Au disc at rotation rates 200 (a), 500 (b), 1500 (c) and 2500 (d) rpm in 1.0 mol dm^{-3} NaOH containing 0.02 mol dm^{-3} NaBH4 at 10 mV s^{-1}.

A Levich analysis (Bard and Faulkner, 2001) (using Eq. 3.3) of the oxidation plateau at -0.05 V shown in Fig. 3.19 revealed a diffusion-controlled reaction and the attainment of near-maximum coulombic efficiency for borohydride oxidation with n=7.49 (Eq. 3.3):

$$Ilim = 0.62nFCD^{2/3} \nu^{-1/6} \Omega^{1/2} \quad \text{(Eq. 3.3)}$$

where the kinematic viscosity (ν) = 1.14×10^{-2} cm^2 s^{-1} and the diffusion coefficient (D) = 1.28×10^{-5} cm^2 s^{-1}.

The Levich plot is shown in Fig. 3.20. The values used for D and ν were those recently determined by Molina Concha et al. (2009) for 10 mM $NaBH_4$ in 1 M NaOH at 25 °C. The n values determined here support those recently determined in an RDE study of BH_4^- oxidation at Au by Finkelstein et al. (2009) where they reported that a 7–8 electrons oxidation of BH_4^- occurs at -0.2 V vs. Ag/AgCl and that the oxidation peak at -0.52 V vs. Ag/AgCl yields 4.5 electrons per molecule with the remainder of the electrons possibly generating hydrogen.

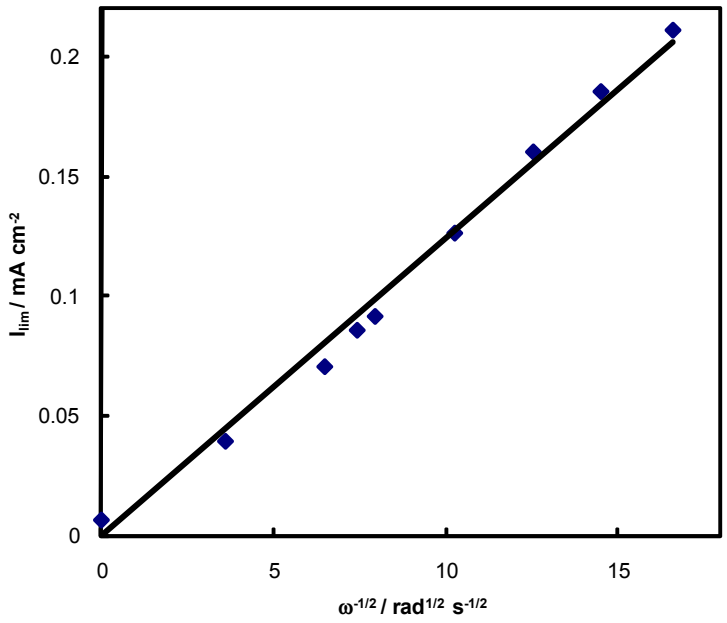

Figure 3.20. Levich plot for NPG-coated gold disc in 1.0 mol dm^{-3} NaOH containing 0.02 mol dm^{-3} $NaBH_4$ at 5 mV s^{-1}.

3.7 Linear Sweep Voltammetry Study at a Series of Nanoporous Gold Electrodes

The linear sweep voltammograms for the oxidation of borohydride at the fabricated NPG electrodes are shown in Fig. 3.21. The current for the oxidation of 20 mM borohydride at the Au disc, Au disc with NPG deposit and NPG wire array at the plateau centred at 0.0 V was measured as 3.17, 25, 38 and 73.6 mA cm^{-2}, respectively. The geometrical area exposed to the electrolyte was used to calculate the current density for each electrode. This equates to a 8-, 12- and 24-fold increase in current at the segmented Au-NPG wire array, Au disc with NPG deposit and NPG wire array, respectively over that recorded at the Au disc. The onset potential for borohydride oxidation shifts from -0.80 V at the Au disc to -0.87 V, -0.95 V and -1.07 V at the segmented NPG-Au wire array, Au disc with NPG deposit and NPG wire array, respectively.

The electrochemically surface areas of the three NPG electrodes were estimated from the charge associated with the gold oxide reduction peak in 1 M NaOH at *ca.* -0.1 V (shown in Fig. 3.15), assuming that the charge/area ratio is usually considered to be *ca.* 400 μC cm^{-2} for a regular polycrystalline Au electrode. The real surface areas were calculated to be 0.197, 610, 1009, 1240 cm^2 for the Au disc, segmented NPG-Au wire array, Au disc with NPG deposit and NPG wire array, respectively. The intrinsic electrode kinetic activity for the oxidation of 20 mM borohydride in 1 M NaOH was calculated as 4.59, 7.52 and 72.1 μA cm^{-2} for the segmented NPG-Au wire array, Au disc with NPG deposit and NPG wire array, respectively. The intrinsic kinetic activity of the NPG electrodes cannot be compared with nanostructured gold-based electrodes from the literature as the electrochemically active surface areas for these are not given. The catalytic activity can be compared **only** to these electrodes based on the reported oxidation current densities determined from the geometric electrode area. The reported oxidation current for 20 mM borohydride in 3M NaOH at 10 mVs-1 at a gold foil, gold nanoparticles supported on titanate nanotubes and E-TEK 10 wt% gold on Vulcan XC72R was 4.5, 10 and 15 mA cm^{-2}, respectively (Ponce-de-León et al., 2006). An oxidation

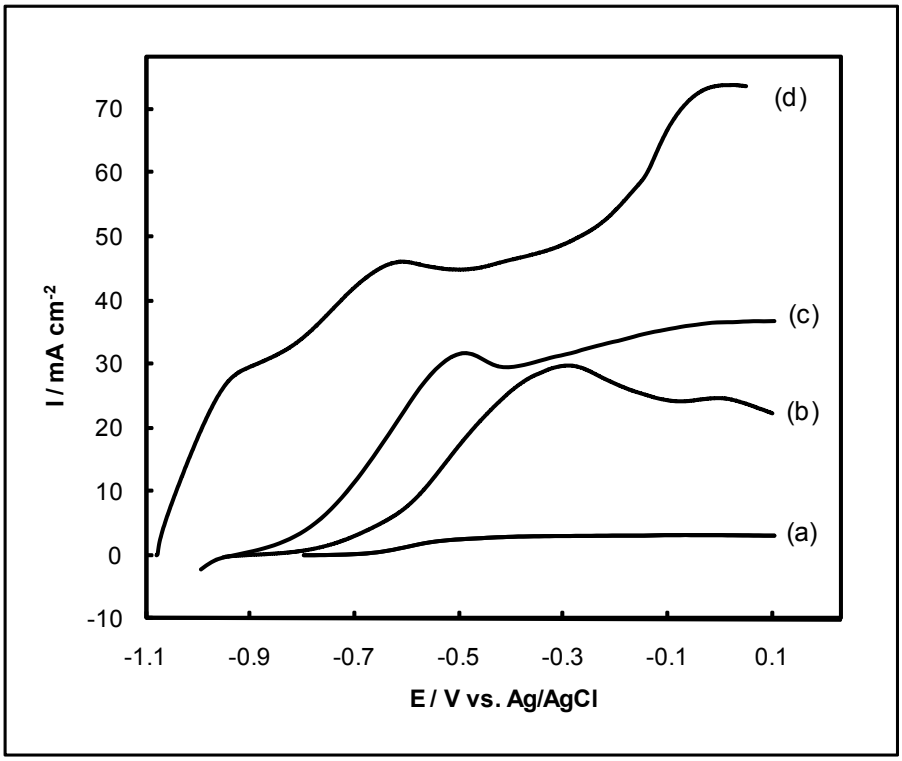

Figure 3.21. Linear sweep voltammetric response for (a) Au disc (b) nanoporous gold (NPG)-Au segmented wire array electrodes (c) nanoporous gold (NPG)-coated Au disc and (d) nanoporous gold (NPG) wire array and in 1.0 mol dm^{-3} NaOH containing 0.02 mol dm^{-3} $NaBH_4$ under static conditions at 10 mV s^{-1}.

current for 100 mM borohydride in 1 M NaOH at 10 mVs^{-1} at carbon-supported gold hollow nanospheres of 57 mA cm^{-2} was reported by Wei et al. (2009). This comparison serves to highlight the superior activity of NPG over other nanostructured gold-based electrodes for borohydride oxidation at similar concentrations.

It is possible that the primary reason that NPG is a more active catalyst for borohydride oxidation reaction (BOR) than bulk planar gold is that intrinsically NPG has a higher step density and hence a greater number of active sites than bulk planar gold. The active sites are defect sites with lower bond coordination numbers. Such sites may aid adsorption of reactants via electronic or steric interactions. It is also possible that the structure of the active layer at NPG promotes an increase in the residence time of BOR reaction intermediates at the surface, leaving more time for complete oxidation to borate. Such behaviour was recently reported by Schneider et al. (2008) for the multi-step oxygen reduction reaction at arrays of Pt nanostructures at planar glassy carbon electrodes.

3.8 The Electrochemistry of Ammonia Borane at Gold

The typical behaviour for Au in 1 M NaOH is seen in the CV recorded for a microdisc electrode shown in Fig. 3.22. This CV shows that negligible current flows in the absence of AB over the potential range −1.0 to +0.05 V. The onset of monolayer oxide formation was shown to occur above +0.05 V with the corresponding oxide reduction peak on the reverse sweep.

When 20 mM AB was added to 1 M NaOH solution, a well-defined CV (shown in Fig. 3.23) was achieved – consisting of two irreversible anodic waves. Mass transport controlled steady-state currents were recorded for the first and second waves at −0.95 and −0.12 V, respectively. The CVs exhibited a pronounced plateau region upon sweeping the potentials to more positive values. The current decreased as the potential was swept into the Au monolayer oxide region.

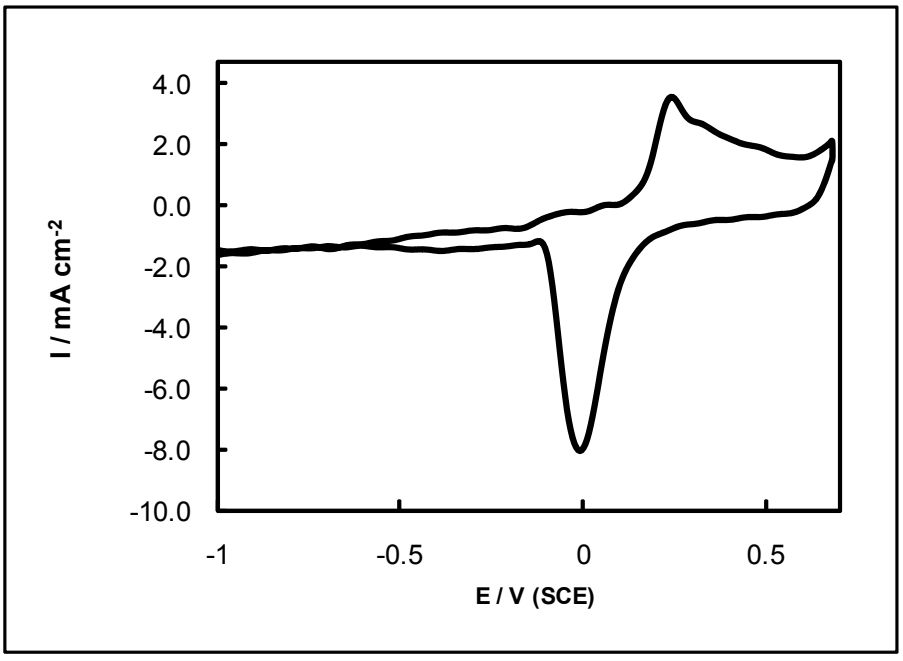

Figure 3.22. Cyclic voltammogram (CV) for Au microdisc (r = 5 µm) in 1.0 mol dm^{-3} NaOH, 10 mV s^{-1}.

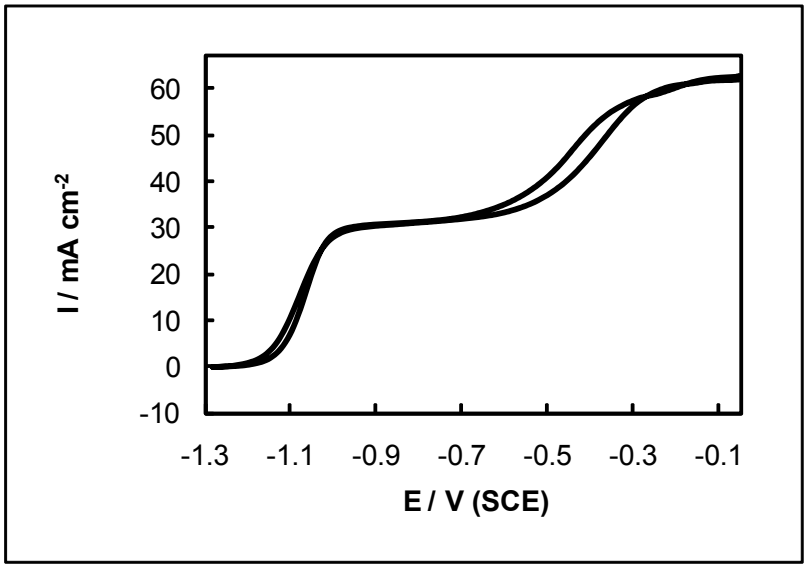

Figure 3.23. Cyclic voltammogram (CV) for an Au microdisc in 1.0 mol dm^{-3} NaOH containing 0.02 mol dm^{-3} AB at 10 mV s^{-1}.

The oxidation response for 20 mM AB in 1 M NaOH solution at a planar Au disc is shown in Fig. 3.24. A single irreversible anodic wave was observed, and it was not possible to resolve this into the two irreversible anodic waves that were recorded at the Au microdisc.

3.9 The Electrochemistry of Ammonia Borane at Nanoporous Gold

The CV response for 20 mM AB in 1 M NaOH solution at NPG on a planar Au disc is shown in Fig. 3.25. The onset potential for the oxidation of AB shifted to a more negative potential of -1.20 V and the oxidation current of 3.1 mA cm^{-2} represents a 24% increase over that seen at an Au disc electrode.

The CV response for 20 mM AB in 1 M NaOH solution at NPG wire array is shown in Fig. 3.26. The onset potential for the oxidation of AB shifted to a more negative potential of -1.30 V and the oxidation current of 13.1 mA cm^{-2} represents more than a fivefold increase over that seen at an Au disc electrode.

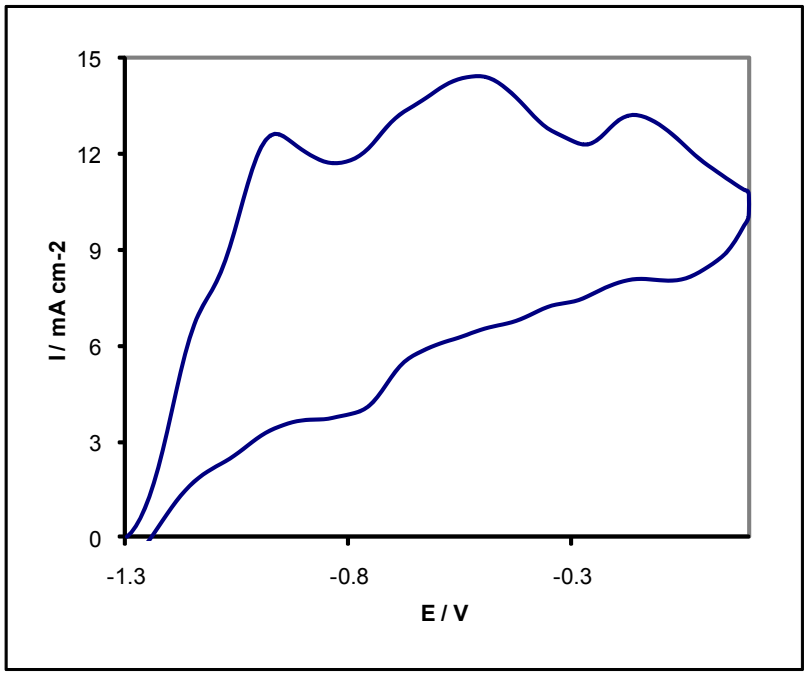

Figure 3.24. Cyclic voltammogram (CV) for an Au disc in 1.0 mol dm^{-3} NaOH containing 0.02 mol dm^{-3} AB at 10 mV s^{-1}.

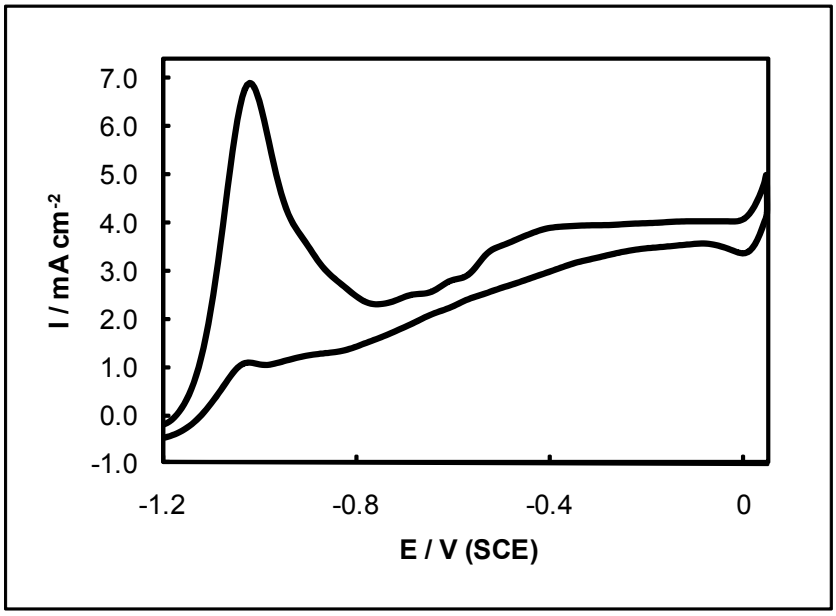

Figure 3.25. Cyclic voltammogram (CV) for nanoporous gold (NPG) on an Au disc electrode in 1.0 mol dm^{-3} NaOH containing 0.02 mol dm^{-3} AB at 10 mV s^{-}.

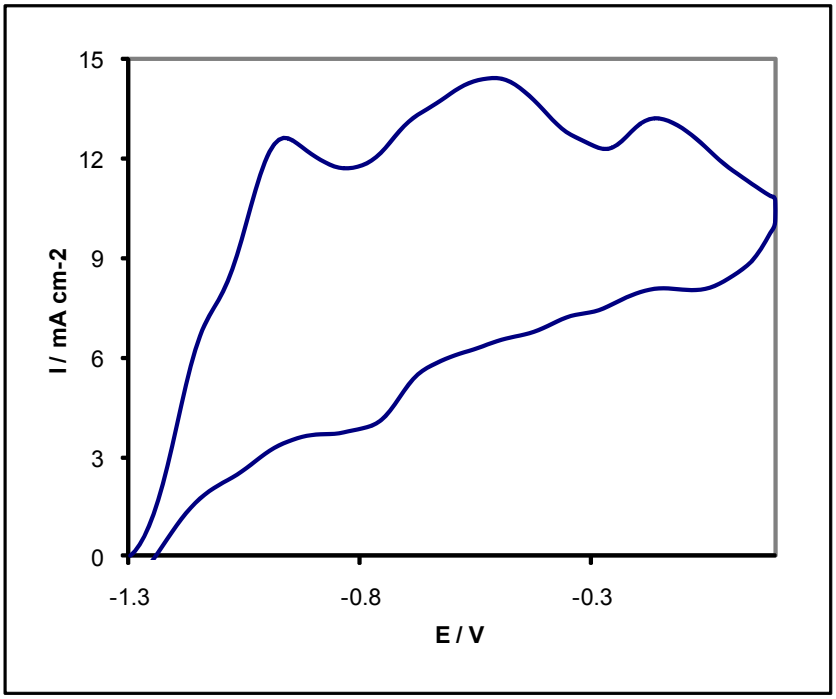

Figure 3.26. Cyclic voltammogram (CV) for nanoporous gold (NPG) wire array in 1.0 mol dm^{-3} NaOH containing 0.02 mol dm^{-3} AB at 10 mV s^{-1}.

The CV response for 20 mM AB in 1 M NaOH solution at segmented NPG-Au wire array is shown in Fig. 3.27. The onset potential for the oxidation of AB is -1.27 V and the oxidation current of 12.8 mA cm^{-2} represents a fivefold increase over that seen at an Au disc electrode.

The CV response for 20 mM AB in 1 M NaOH solution at a NPG-coated Au array is shown in Fig. 3.28. The onset potential for the oxidation of AB has shifted to a more negative potential of -1.20 V and the oxidation current of 10.5 mA cm^{-2} represents more than a fourfold increase over that seen at an Au disc electrode.

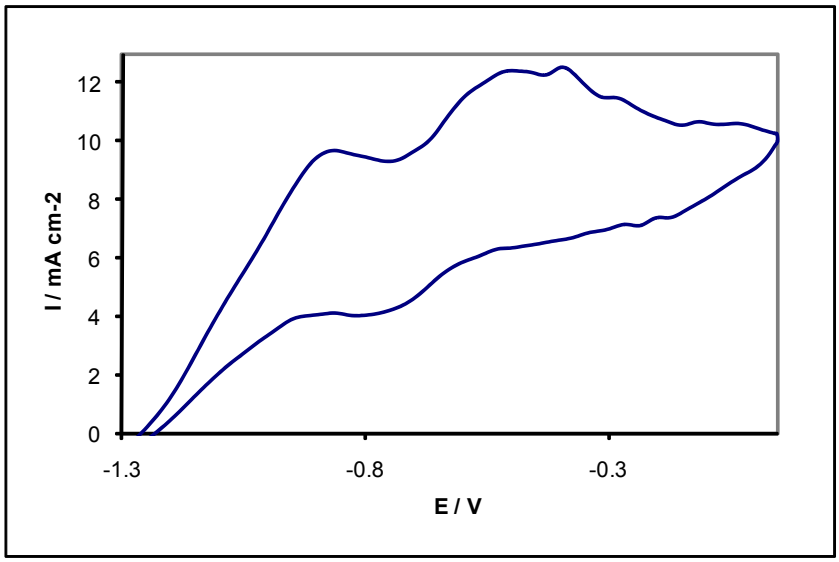

Figure 3.27. Cyclic voltammogram (CV) for segmented nanoporous gold (NPG)-Au wire array in 1.0 mol dm^{-3} NaOH containing 0.02 mol dm^{-3} AB at 10 mV s^{-1}.

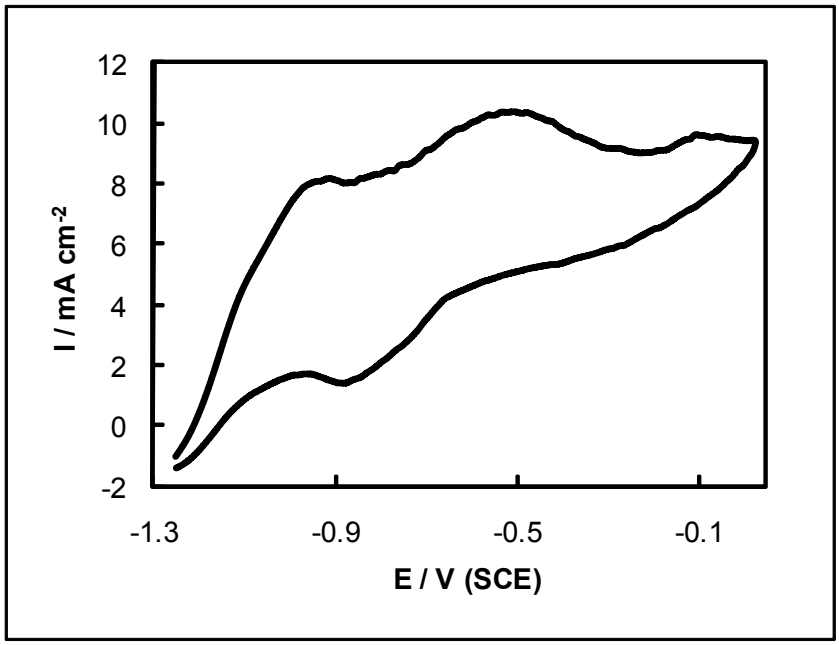

Figure 3.28. Cyclic voltammogram (CV) for NPG-coated Au wire array on a planar Au film in 1.0 mol dm^{-3} NaOH containing 0.02 mol dm^{-3} AB at 10 mV s^{-1}.

The higher oxidation current for AB at NPG and the lower onset potential for the oxidation relative to planar bulk gold indicates that NPG is a more effective catalyst for the reaction. This is in agreement with the behaviour seen for borohydride at NPG.

3.10 Assembly of a Prototype Direct Borohydride Fuel Cell

A DBFC 1cm^2 in size with active electrode area composing of printed circuit board (PCB) plates fabricated inhouse was used to test the efficiency of NPG as an anode material.

3.10.1 Prototype Direct Borohydride Fuel Cell Anode

The anode was fabricated by depositing NPG on a silicon wafer with a 200 nm gold layer. Gold was deposited by e-beam evaporation using the TEMESCAL. The anode was secured to the PCB plates using a silicone sealant that was allowed to dry overnight at room temperature.

3.10.2 Prototype Direct Borohydride Fuel Cell Cathode

The cathode material was sourced commercially. The cathode was applied to a gas diffusion layer (GDL). The GDL was fabricated according to the following steps:

1 Sonicate carbon black, polytetrafluoroethylne and isopropyl alcohol for 2 hours to give a slurry;

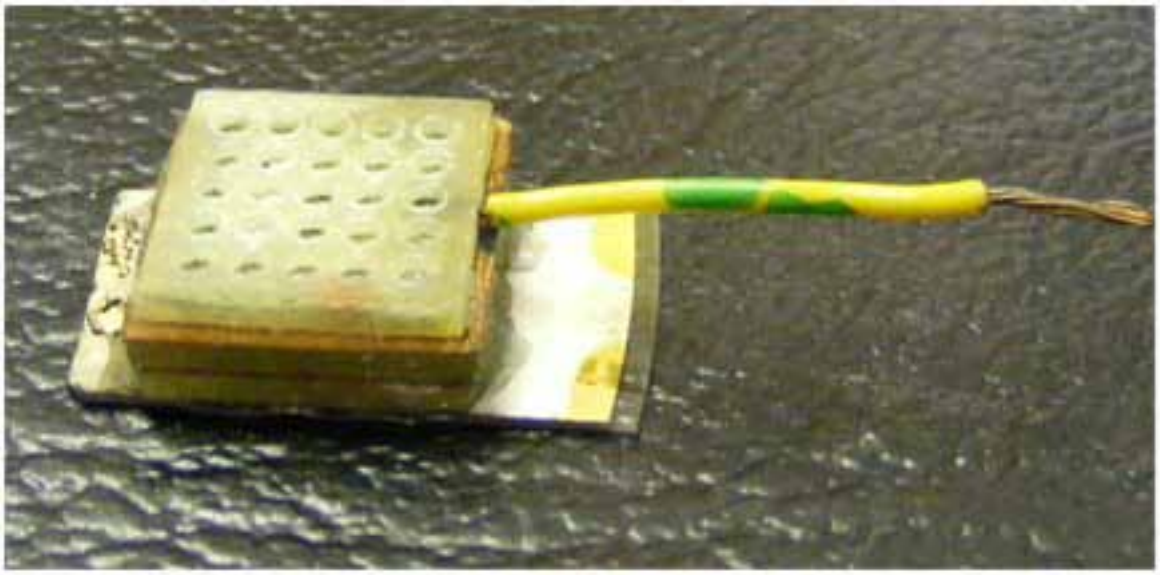

Figure 3.29. Side view of direct borohydride fuel cell (DBFC).

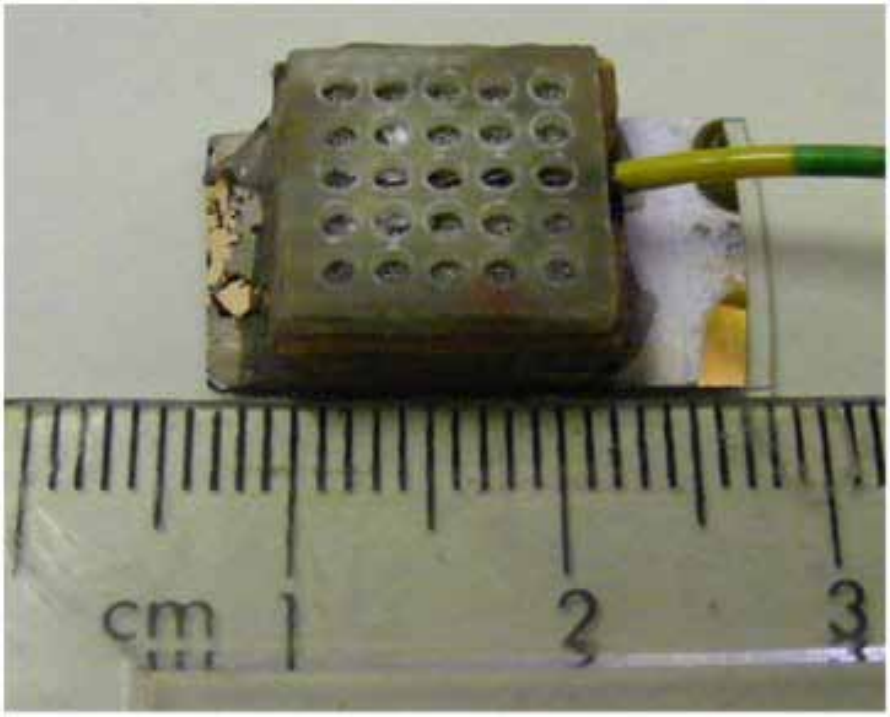

Figure 3.30. Top-down view of direct borohydride fuel cell (DFBC).

2 Brush the resulting coating on Ni foam;

3 Dry and press manually in between PCB plates;

4 Sinter for 30 minutes.

The entire active cathode catalyst was assembled according to the following steps:

1 Sonicate carbon black, PTFE, MnO_2 and Isopropyl alcohol to give a slurry MnO_2 dispersed on carbon;

2 Brush the resulting coating on GDL;

3 Dry in oven and press manually in between PCB plates;

5 Sinter for 30 minutes.

The entire DBFC is shown in Figs 3.29–3.30.

3.10.3 Performance of Prototype Direct Borohydride Fuel Cell

The cell was tested using 20 mM borohydride in 2 M NaOH. An open circuit potential of 0.66 V was recorded. The polarisation curve shown in Fig. 3.31 was constructed based on a multi-potential step analysis of the current output from the cell. A maximum current density of 3.0 mA cm^{-2} was recorded at a voltage of 0.20 V. The maximum power density recorded was 0.63 mW cm^{-2} at 0.25 V. The DBFC was tested also at 75 mM borohydride in 2 M NaOH. The maximum current recorded was 5.1 mA cm^{-2} at 0.10 V. The maximum power density recorded was 0.65 mW cm^{-2} at 0.25 V.

Four additional fuel cells with 1 cm^2 sized active area are being fabricated which will be connected in a series with the existing cell to yield a higher net output voltage and current. Higher fuel concentrations are also being tested.

An NPG wire array integrated on silicon was fabricated for testing as an alternative anode to the above NPG film on silicon. It was anticipated that this would yield a higher output current and power density. NPG was deposited in a silicon-integrated alumina template. The procedure established for the formation of this template involved the following steps:

1 One-step anodisation of Al/Au/Si substrate with Ti adhesion layers in 0.3 M oxalic acid. The metal layers were 3 micron thick Al and 200 nm thick Au with intervening Ti adhesion layers of 20 nm thickness. The layers were deposited consecutively by e-beam evaporation using the TEMESCAL evaporator;

2 Ten minutes 5 wt% H_3PO_4 etch to complete barrier layer removal and widen pores.

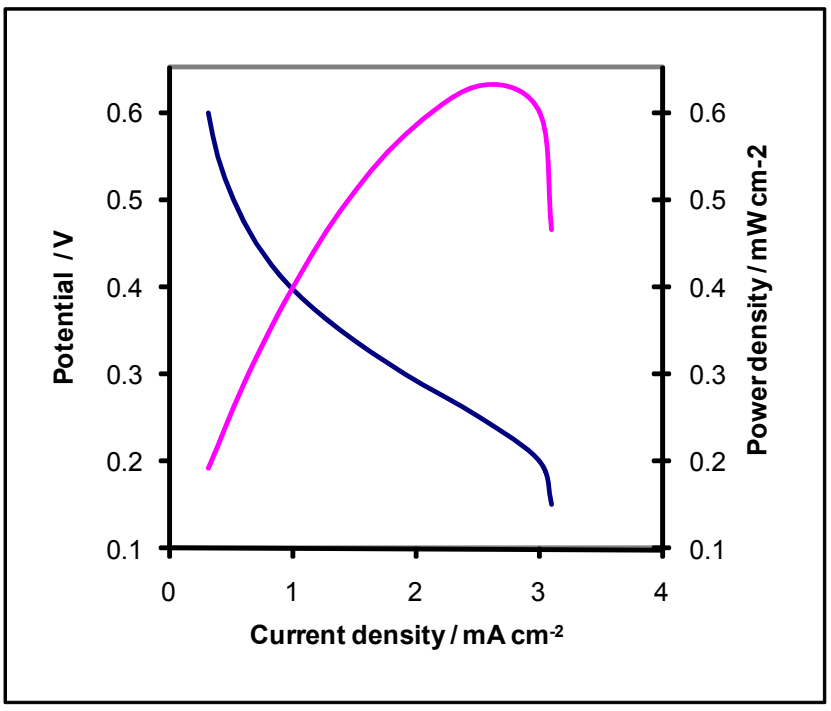

Figure 3.31. Polarisation curve for direct borohydride fuel cell (DBFC) with 20 mM borohydride in 2 M NaOH at room temperature.

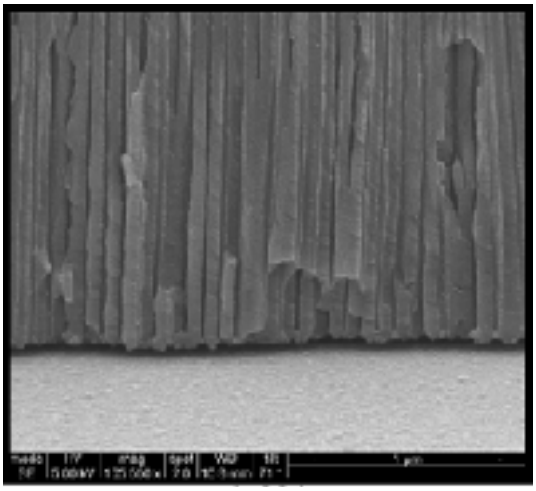

Figure 3.32. Scanning electron micrograph (SEM) image of alumina template on Si wafer.

The template obtained is shown in the SEM image in Figure 3.32. The pore size of the alumina template can be tuned by varying the etch time in 5 wt % H_3PO_4.

However, preliminary tests showed that when a NPG wire array was tested as an anode in the prototype DBFC it did not outperform a NPG film. Further work is required to optimise this process which should lead to an enhancement in DBFC performance.

4 Relevance of the Project to Policy and Legislation

4.1 Legislative Drivers

An innovative energy policy is key to the EU 2020 strategy for sustainable growth. Measures taken to decarbonise the transport and energy sector are critical in ensuring long-term sustainability. Establishing an efficient, secure and low-carbon economy requires targeted investment in the development and deployment of innovative and low-carbon technologies in future transport and energy systems. Fuel cells and hydrogen technology play a central role in the EU's shift towards an efficient low-carbon economy. Fuel cells and hydrogen technology are linked to the four large-scale initiatives announced in the EU Energy 2020 Communication – *Smart Grids, Energy Storage, Large-scale Biofuel production, Smart Cities* (de Colvenaer, 2011).

Fuel cells represent a clean and highly efficient power source applicable across a wide range of industries, including automobiles, large-scale back-up power systems, decentralised power generation in buildings and portable electronics. Various applications are already becoming cost competitive and many will reach commercial status this decade. Fuel cell vehicles could be cost competitive with conventional internal combustion engine cars by 2025, provided the right incentives are in place and an appropriate refuelling infrastructure is built (Reis, 2010). When combined either with hydrogen or as part of a combined heat and power (CHP) system, fuel cells play an important role in optimising smart grid efficiency and reducing emissions. They enable end-users to generate their own electricity at the location where it is required and/ or reduce CO_2 emissions from existing plants. Reducing energy consumption in urban areas is a key target for achieving low-carbon emissions in EU member states, and increasing energy efficiency in buildings is one of the main drivers. The other main driver is decarbonising urban transport. Fuel cell systems represent a vital part of the solution in reducing CO_2 and other polluting emissions. Continuous investments are needed in research, development and demonstration (RD&D) and market deployment to unleash the vast potential of fuel cell and hydrogen technology. The Joint Undertaking for Fuel Cell and Hydrogen Technology (FCH JU), set up as the first European Industrial Initiative (EII) under the EU Strategic Energy Technology Plan (SET Plan, European Commission, 2007), covers just part of this RD&D need for a limited time frame (up to 2013). The EU's SET Plan has the objective of accelerating innovation in cutting-edge European low-carbon technologies. The plan strives to deliver affordable and competitive low-carbon technologies. It will facilitate the achievement of the 2020 targets and the 2050 vision of the Energy Policy for Europe. The plan focuses on measures relating to planning, implementation, resources and international cooperation in the field of energy technology. The SET Plan includes:

- The European Industrial Bioenergy Initiative;
- The European CO_2 Capture, Transport and Storage Initiative;
- The European Electricity Grid Initiative;
- The Fuel Cells and Hydrogen (FCH) Joint Technology Initiative;
- The Sustainable Nuclear Initiative;
- Energy Efficiency – The Smart Cities Initiative;
- The Solar Europe Initiative;
- The European Wind Initiative;
- The SET-Plan Steering Group (SET-Group);
- The European Energy Research Alliance (EERA);
- The SET-Plan Information System (SETIS).

For the commercialisation of fuel cell applications over the next decade, the integration of fuel cell activities in current and future EU energy and transport financing schemes, envisaged in FP 8, TEN T, Structural Funds and the Innovation Union, is crucial to avoid expensive 'make-overs' at a stage when applications come to market.

4.2 Fuel Cell Technology including Industry Status and Associated Barriers to Deployment

Proton exchange membrane technologies (PEMFC), molten carbonate fuel cell (MCFC) and solid oxide fuel cell (SOFC) are the three main technologies of fuel cells currently under development for transport and stationary applications in Europe (European Commission, 2007).

The main focus for PEMFC are automotive applications; MCFC and SOFC are focused mainly on industrial and residential applications. By 2015 a fuel consumption of 0.27 kWh/km is expected for PEMFC-based transport vehicles running on hydrogen, which is almost 40% lower fuel consumption than an advanced internal combustion engine for a similar vehicle size. The development of cost-competitive hydrogen storage technologies is key for all applications. Hydrogen has a very high-energy content by weight (120 MJ/kg ~ ca. three times that of gasoline) but very low energy content by volume (8 MJ/l) (four times less than gasoline). Therefore, hydrogen needs to be compressed to increase its energy content by volume so as to provide an economically viable hydrogen storage solution. The three main media used in storing hydrogen are compressed hydrogen gas tanks, liquid hydrogen tanks and chemical hydrogen storage. Hydrogen storage is regarded as a 'grand challenge' (United States Department of Energy, 2011).

The challenge pertains most directly to the transportation applications, where storage capacity, energetics, form factor and performance requirements have yet to be satisfied technically and economically. There has been steady progress, however, and the focus is clearly on solid materials as the preferred storage medium to enable a greater driving range for transportation applications. As liquid and gas storage options are limited in their potential to meet longer-term goals, new materials and solutions are needed to meet this challenge. A light-duty hydrogen-based fuel cell vehicle must carry *ca.* 5–13 kg of hydrogen on board to allow a driving range of 300 miles. Using currently available storage technology, placing a sufficient quantity of hydrogen on board a vehicle would require a tank larger than the trunk of a typical car, the weight of which would reduce fuel economy. At present, gaseous and liquefied technologies are commercially available. An increase in the tank operating pressure, and a reduction of the boil-off rate for liquefied storage are the main development trends. Gaseous hydrogen storage tanks at 70 MPa are currently in the demonstration stage. A medium-cost target (about 2020) is around €10 to 30/kWhH2, that is a decrease by about a factor 3 to 10 with respect to currently available technologies. To meet all these targets, alternative solid-state hydrogen storage technologies are being developed, still requiring further research. The market entry of the latter technologies is expected post-2020.

Combined heat and power is the targeted means of energy conversion for fuel cells in stationary applications. Hydrocarbon fuels (natural gas, biofuels) are expected to be the dominant fuel up to 2030. Molten carbonate fuel cells are currently the most mature technology available for demonstration/commercial projects above 100 kWe; overall energy efficiencies of 75% to 80% have been achieved with a cumulative running time of 10 000–20 000 hours. Proton exchange membrane technologies have been developed and tested mostly below 50 kWe with electrical efficiencies of around 30–40%. Solid oxide fuel cell technologies are mainly at the prototype demonstration stage. The capital investment for stationary fuel cell applications is estimated to be €1000–€1500/kWe with overall energy efficiencies of 90%, by 2015–2020 for sizes above 100 kWe with a medium-term lifetime goal above 30 000 hours.

Cost and durability are the major barriers to hydrogen penetration as a fuel in the transport sector and for stationary applications. For both hydrogen production and fuel cell technologies, significant research and demonstration is still needed on materials, process integration to meet customer performance requirements and to lower system costs. The supply–demand investment dilemma for the infrastructure build-up poses another barrier facing the hydrogen-energy economy. For transportation needs, 10 to 20% of retail stations will have to deliver hydrogen once hydrogen-fuelled cars are significantly introduced. Many EU companies that have been established in the fuel-cell business are small and medium enterprises, and such companies face an equity dilemma. Support for these companies is vital in market establishment phases (European Commission, 2007).

4.3 Environmental Protection Agency Activities that Influence the Energy Sector

- The Environmental Protection Agency (EPA) has responsibility for producing national greenhouse gas and air emissions inventories, as well as inventories for acidifying gases and ozone precursors. These inventories are used nationally and internationally to inform air, climate and energy policies.
- The EPA licenses the operation of power-generation plants and each licence application is considered on its merits.
- The EPA has responsibility for implementing the EU's Emissions Trading Scheme in Ireland, which is a policy measure targeted at large producers of carbon dioxide, to reverse the growth in greenhouse gas emissions. The Emissions Trading Scheme creates further incentives for power companies to improve energy efficiency and diversify into carbon-neutral renewable energy sources.
- Through its *State of the Environment* reports the EPA has supported the development of renewable energy, which has significant environmental benefits compared to fossil fuel sources. The EPA's view is that all development (energy or otherwise) should protect the natural environment while taking into account the environmental, social and economic principles of sustainable development.
- The energy sector is one of the designated sectors where competent authorities must subject specific plans and programmes to a strategic environmental assessment (SEA). The objective of an SEA is to provide for a high level of protection of the environment and to promote sustainable development.

In addition, the Irish government's Science strategy, *Strategy for Science, Technology and Innovation* (Department of Enterprise, Trade and Employment, 2006) has recognised that high levels of investment in research and innovation are essential both for economic competitiveness and to yield innovations in areas such as environmental technologies which make tangible improvements to our quality of life.

5 Conclusions and Recommendations

Borohydride oxidation was studied by cyclic voltammetry at NPG in a range of architectures. The onset potential for borohydride oxidation at NPG was found to shift to more negative potentials than that observed at bulk Au. The onset potential shifted from -0.80 V at an Au disc to -0.87 V, -0.95 V and -1.07 V vs. Ag/AgCl at a segmented NPG-Au wire array, Au disc with NPG deposit and NPG wire array, respectively. The oxidation current for 20 mM borohydride in 1 M NaOH increased from 3.17 at an Au disc to 25, 38 and 73.6 mA cm^{-2} at a segmented NPG-Au wire array, Au disc with NPG deposit and NPG wire array, respectively. Comparison of the activity of NPG for borohydride oxidation with other nanostructured gold-based electrodes reported in the literature highlighted the superior activity of NPG.

NPG presents an attractive alternative to gold nanoparticle-based catalysts for fuel cells as it does not require a carbon support, thereby removing the stability issues associated with these. NPG may be incorporated as a thin foil as a porous catalyst electrode as it is shapable and has high mechanical, thermal and chemical stability coupled to high catalytic activity. It has a dual functionality in that it can act as a current collector and as a catalyst. NPG may be integrated into nafion-based MEAs in conventional PEM fuel cells. An example of a PEM fuel cell using Pt modified NPG was demonstrated by Erlebacher et al. (2007). An advantage of incorporating NPG over platinum in fuel cells would be the useful enhancement in electrical conductivity that could be derived due to the lower electrical resistivity of gold. NPG can provide a solution to the sintering problems that plague nanoparticle-based catalysts and allows for more intimate contact with an electrical substrate to be established. The porous structure promotes mass transport of the reactant to the active sites and release of gaseous by-products. The diffusion of an electroactive species to gold nanoparticles on a high surface area carbon support is limited by the low degree of porosity of the support.

In summary, the facile and efficient oxidation of this high-energy density fuel at NPG which does not emit carbon by-products points to the future integration of this catalyst in the anode compartment of a DBFC. In order to realise the full potential of decarbonised energy technologies the efficient oxidation of zero carbon fuel sources must be developed.

6 References

Amendola, S.C., Onnerud, P., Kelly, M.T., Petillo, P.J., Sharp-Goldman, S.L. and Binder, M, 1999, A novel high power density borohydride-air cell. *Journal of Power Sources* 84: 130–3.

Bard, A.J and Faulkner, L.R. 2001, *Electrochemical Methods*, John Wiley and Sons, Inc.: New York, 2nd edn.

Barrett, S., 2005, Direct borohydride fuel cell technology for PCs. *Fuel Cells Bulletin*, 9–10.

Biener, J., Hodge, A.M., Hayes, J.R., Volkert, C.A., Zepeda-Ruiz, L.A., Hamza, A.V., and Abraham, F.F., 2006, Size effects on the mechanical behaviour of nanoporous Au. *Nano Letters* 6(10): 2379–82.

Cameron, D.S., 2006, The Ninth grove Fuel Cell Symposium – Building and commercialisation of a fuel cell industry. *Platinum Metals Review* 50(1): 38–45.

Chatenet, M., Micoud, F., Roche, I. and Chainet, E., 2006, Kinetics of sodium borohydride direct oxidation and oxygen reduction in sodium hydroxide electrolyte BH_4^- electro oxidation on Au and Ag catalysts. *Electrochimica Acta* 51: 5452–8.

Chatenet, M., Molina-Concha, B., Diard, J.P., 2009, First insights into the borohydride oxidation reaction mechanism on gold by impedance spectroscopy. *Electrochimica Acta* 54:1687–93.

Choudhary, T.V. and Goodman, D.W., 2005, Catalytically active gold: The role of cluster morphology. *Applied Catalysis A* 291: 32–6.

De Colvenaer, B. (2011) *Hydrogen and Fuel Cell Technology are an Essential Element for Transforming to a Smart, Low Carbon and Secure EU Energy System*, www.fchindustry-jti.eu/documents/JOINTFCH positionpaperfinal31.01.2011.pdf

Delahay, P. (1954). *New Instrumental Methods in Electrochemistry*, Interscience, New York.

Department of Enterprise, Trade and Employment (2006) *Strategy for Science, Technology and Innovation* http://www.djei.ie/publications/science/2006/sciencestrategy.pdf

Erlebacher, J., Zeis, R., Mathur, A., Fritz, G., Lee, J., 2007, Platinum-plated nanoporous gold: An efficient low Pt loading electrocatalyst for PEM fuel cells. *Journal of Power Sources* 165: 65–72.

European Commission (2007) *A European Strategic Energy Technology Plan (SET-Plan)*¸available at: http://ec.europa.eu/energy/technology/set_plan/doc/2007_technology_map_description.pdf

European Environment Agency, 2006, *Report on Environment and Human Health*, No. 10/2005, European Environment Agency, p. 6.

Finkelstein, D.A., Nicolas, D.M., Cohen, J.L., Abruna, H.D., 2009, Rotating Disk Electrode (RDE) Investigation of BH_4^- and BH_3OH^- Electro-oxidation at Pt and Au: implications for BH_4^- fuel cells. *Journal of Physical Chemistry* C 113(45): 19700–12.

Forty, A.J., 1979, Corrosion micromorphology of noble metal alloys and depletion gilding. *Nature* 282: 597–8.

Indig, M.E. and Snyder, R.N., 1962, Sodium borohydride, An Interesting Anodic Fuel. J. Electrochem. Soc. 109: 1104–6.

Jacobson, M.Z., Colella, W.G. and Golden, D.M., 2005, Switching to a U.S. hydrogen fuel cell vehicle fleet: The resultant change in emissions, energy use, and greenhouse gases. *Science* 308: 1901–5.

Krishnan, P., Yang, T., Advani, S.G. and Prasad, A., 2008, Rotating ring-disc electrode (RRDE) investigation of borohydride electro-oxidation. *Journal of Power Sources* 182:106–11.

Leon, C.P.D., Walsh, F.C., Pletcher, D., Browning, D.J. and Lakeman, J.B., 2006, Direct borohydride fuel cells. *Journal of Power Sources* 155: 172–81.

Liu, B. and Suda, S., 2008, Development of high-performance planar borohydride fuel cell modules for portable applications. *Journal of Power Sources* 175: 226–31.

Liu, L. and Scholz, R., 2008, Fabrication and characterization of a flow-through nanoporous gold nanowire/AAO composite membrane. *Nanotechnology* 19: 335604–10.

Molina Concha, B., Chatenet, M., El-Kissi, N., Parrour, G., Diard, J.P., 2009, Direct rotating ring-disk measurement of the sodium borohydride diffusion coefficient in sodium hydroxide solutions. *Electrochimica Acta* 54: 4426–35.

Pattricka, G., van der Lingen, E., Corti, C.W., Holliday, R.J., Thompson, D.T., 2004, The potential for use of gold in automotive pollution control technologies: a short review. *Topics in Catalysis* 30: 273–9.

Pickering, H.W., 1983, Characteristic Features of Alloy Polarization Curves. *Journal of Corrosion Science* 23: 1107–20.

Ponce-de-León, C., Bavykin, D.V., Walsh, F.C., 2006, The oxidation of borohydride at titanate nanotube supported gold electrodes. *Electrochemistry Communications* 8: 1655–60.

Reis, A. (2010) *A Portfolio of Power-trains for Europe: A Fact-based Analysis*, Zero Emissions Vehicles, European Union, www.zeroemissionvehicles.eu

Schneider, A., Colmenares, L., Seidel, Y.E., Jusys, Z., Wickman, B., Kasemo, B., Behm, R.J., 2008, Transport effects in the oxygen reduction reaction on nanostructured, planar glassy carbon supported Pt/GC model electrodes. *Physical Chemistry Chemical Physics* 10: 1931–43.

Searson, P. and Ji, C., 2003, Synthesis and Characterization of Nanoporous Gold Nanowires. *J Physical Chemistry B* 107: 4494–9.

Sieradzki, K. and Karma, A., 2001, Evolution of nanoporosity in dealloying. *Nature* 410: 450–3.

Steele, B.C.H., Heinzel, A., 2001, Materials for fuel-cell technologies. *Nature* 414: 345–52.

Tian, F. and Xu, C. J., 2007, Low Temperature CO Oxidation over Unsupported Nanoporous Gold. *Journal of the American Chemical Society* 129: 42–3.

United States Department of Energy (2011) the National Hydrogen Storage Project, US Department of Energy, http://www1.eere.energy.gov/hydrogenandfuelcells/storage/national_proj.html.

Wang K., and Chen G., 2008. Eight-Electron Oxidation of Borohydride at Potentials Negative to reversible hydrogen electrode. *Journal of Power Sources* 185: 892–4.

Wee, J.H., 2006, Which type of fuel cell is more competitive for portable application: Direct methanol fuel cells or direct borohydride fuel cells. *Journal of Power Sources* 161: 1–10.

Wei J., Wang X., Wang Y., Chen Q., Pei F., Wang Y., 2009, Investigation of carbon-supported Au hollow nanospheres as electrocatalyst for electrooxidation of sodium borohydride. *International Journal of Hydrogen Energy* 34: 3360–6.

Zielasek, V., Jurgens, B., Schulz, C., Biener, J., Biener, M., Hamza, A.V. and Baumer, M. 2006, Nanoporous Gold Foams. *Angewandte Chemie International Edition* 45: 8241–4.

Zeis, R., 2008, Catalytic reduction of oxygen and hydrogen peroxide by nanoporous gold. *Journal of Catalysis* 253: 132–8.

Acronyms

DBFC	Direct borohydride fuel cell
MEA	Membrane electrode assemblies
CEM	Cation-exchange membrane
CV	Cyclic voltammogram
DMFCs	Direct methanol fuel cells
EDX	Elemental detection analysis
MCFC	Molten carbonate fuel cell
NPG	Nanoporous gold
PEM	Polymer electrolyte membrane
PEMFC	Proton exchange membrane fuel cell
SEM	Scanning electron micrograph
SOFC	Solid oxide fuel cell
TEM	Transmission electron micrograph
XRD	X-ray diffraction

Project Outputs

Publications

Direct oxidation of ammonia borane at nanoporous gold arrays, Lorraine Nagle and James Rohan, 2011, *J. Electrochem Soc*. 157(8) B772-B778

Nanoporous gold anode catalyst for direct borohydride fuel cell, 2011, Lorraine Nagle and James Rohan, *International Journal of Hydrogen Energy*, 36;10319 –10326.

Direct oxidation of ammonia borane at nanoporous gold arrays, Lorraine Nagle and James Rohan, (Manuscript in preparation) *J. Electrochem Soc*.

Nanoporous gold: active catalyst for borohydride and borane oxidation in gold oxide region, Lorraine Nagle and James Rohan (Manuscript in preparation) *Electrochem. Comm*.

Nanoporous gold catalyst for direct borohydride fuel cell, Lorraine Nagle and James Rohan (2008). *Book of abstracts for the 14th International Conference on Solid Films and Surfaces*, 344.

Zero Carbon emission micro fuel cell design, Lorraine Nagle and James Rohan (2011)

State of Knowledge Report, http://erc.epa.ie/safer/iso19115/displayISO19115.jsp?isoID=144

Presentations and Posters

Nanoporous gold anode catalyst for Direct Borohydride Fuel Cell, L. Nagle and J. Rohan. Third European Fuel Cell Technology & Applications 'Piero Lunghi Conference', Rome, 15–18 December 2009, oral presentation.

Direct Oxidation of Ammonia Borane as an Alternative Fuel at Nanoporous Gold, L. Nagle and J. Rohan. ECS meeting, Vienna, 5 October 2009, oral presentation.

Direct Borohydride Fuel Cell – Zero-emission Energy Technology, L. Nagle and J. Rohan. Environmental Research Conference 'Today's Environmental Research; Tomorrow's Environmental Protection', Dublin, 14 November 2008.

Direct Borohydride Fuel Cell – Zero-emission Energy Technology', L. Nagle and J. Rohan. Environmental Research Conference, 12–13 November 2009, Dublin.

Direct Borohydride Fuel Cell – Zero-emission Energy Technology, L. Nagle and J. Rohan. Inspire BioNano International Conference, Nano Green sub theme. 15–16 October 2009, Dublin.

Direct Borohydride Fuel Cell – Zero-emission Energy Technology, L. Nagle and J. Rohan. EPA Masterclass; 19 June 2009 in the Environmental Research Institute , University College Cork.

Micro fuel cell catalysts on silicon substrates, L. Nagle and J. Rohan. Presented at the University of Notre Dame-Queen's University of Belfast-Tyndall National Institute workshop, 21–22 July 2008, Tyndall National Institute, Cork, Ireland.

Nanoporous Gold Catalyst for Direct Borohydride Fuel Cell, L. Nagle and J. Rohan. 14th International Conference on Solid Films and Surfaces, 30 June–3 July 2008, Trinity College Dublin.

Direct Borohydride Fuel Cell – Zero-emission Energy Technology, L. Nagle and J. Rohan. Environmental Research Conference 'Today's Environmental Research; Tomorrow's Environmental Protection', 6–7 February 2008, Royal Kilmainham Hospital, Dublin.

Achievements

Nominated for 'One to Watch' award 2009 by Enterprise Ireland based on research in fuel cell technology.

An Ghníomhaireacht um Chaomhnú Comhshaoil

Is í an Gníomhaireacht um Chaomhnú Comhshaoil (EPA) comhlachta reachtúil a chosnaíonn an comhshaol do mhuintir na tíre go léir. Rialaímid agus déanaimid maoirsiú ar ghníomhaíochtaí a d'fhéadfadh truailliú a chruthú murach sin. Cinntímid go bhfuil eolas cruinn ann ar threochtaí comhshaoil ionas go nglactar aon chéim is gá. Is iad na príomh-nithe a bhfuilimid gníomhach leo ná comhshaol na hÉireann a chosaint agus cinntiú go bhfuil forbairt inbhuanaithe.

Is comhlacht poiblí neamhspleách í an Ghníomhaireacht um Chaomhnú Comhshaoil (EPA) a bunaíodh i mí Iúil 1993 faoin Acht fán nGníomhaireacht um Chaomhnú Comhshaoil 1992. Ó thaobh an Rialtais, is í an Roinn Comhshaoil, Pobal agus Rialtais Áitiúil.

ÁR bhFREAGRACHTAÍ

CEADÚNÚ

Bíonn ceadúnais á n-eisiúint againn i gcomhair na nithe seo a leanas chun a chinntiú nach mbíonn astuithe uathu ag cur sláinte an phobail ná an comhshaol i mbaol:

- áiseanna dramhaíola (m.sh., líonadh talún, loisceoirí, stáisiúin aistrithe dramhaíola);
- gníomhaíochtaí tionsclaíocha ar scála mór (m.sh., déantúsaíocht cógaisíochta, déantúsaíocht stroighne, stáisiúin chumhachta);
- diantalmhaíocht;
- úsáid faoi shrian agus scaoileadh smachtaithe Orgánach Géinathraithe (GMO);
- mór-áiseanna stórais peitreail;
- scardadh dramhuisce.

FEIDHMIÚ COMHSHAOIL NÁISIÚNTA

- Stiúradh os cionn 2,000 iniúchadh agus cigireacht de áiseanna a fuair ceadúnas ón nGníomhaireacht gach bliain.
- Maoirsiú freagrachtaí cosanta comhshaoil údarás áitiúla thar sé earnáil - aer, fuaim, dramhaíl, dramhuisce agus caighdeán uisce.
- Obair le húdaráis áitiúla agus leis na Gardaí chun stop a chur le gníomhaíocht mhídhleathach dramhaíola trí comhordú a dhéanamh ar líonra forfheidhmithe náisiúnta, díriú isteach ar chiontóirí, stiúradh fiosrúcháin agus maoirsiú leigheas na bhfadhbanna.
- An dlí a chur orthu siúd a bhriseann dlí comhshaoil agus a dhéanann dochar don chomhshaol mar thoradh ar a ngníomhaíochtaí.

MONATÓIREACHT, ANAILÍS AGUS TUAIRISCIÚ AR AN GCOMHSHAOL

- Monatóireacht ar chaighdeán aeir agus caighdeáin aibhneacha, locha, uiscí taoide agus uiscí talaimh; leibhéil agus sruth aibhneacha a thomhas.
- Tuairisciú neamhspleách chun cabhrú le rialtais náisiúnta agus áitiúla cinntí a dhéanamh.

RIALÚ ASTUITHE GÁIS CEAPTHA TEASA NA HÉIREANN

- Cainníochtú astuithe gáis ceaptha teasa na hÉireann i gcomhthéacs ár dtiomantas Kyoto.
- Cur i bhfeidhm na Treorach um Thrádáil Astuithe, a bhfuil baint aige le hos cionn 100 cuideachta atá ina mór-ghineadóirí dé-ocsaíd charbóin in Éirinn.

TAIGHDE AGUS FORBAIRT COMHSHAOIL

- Taighde ar shaincheisteanna comhshaoil a chomhordú (cosúil le caighdéan aeir agus uisce, athrú aeráide, bithéagsúlacht, teicneolaíochtaí comhshaoil).

MEASÚNÚ STRAITÉISEACH COMHSHAOIL

- Ag déanamh measúnú ar thionchar phleananna agus chláracha ar chomhshaol na hÉireann (cosúil le pleananna bainistíochta dramhaíola agus forbartha).

PLEANÁIL, OIDEACHAS AGUS TREOIR CHOMHSHAOIL

- Treoir a thabhairt don phobal agus do thionscal ar cheisteanna comhshaoil éagsúla (m.sh., iarratais ar cheadúnais, seachaint dramhaíola agus rialacháin chomhshaoil).
- Eolas níos fearr ar an gcomhshaol a scaipeadh (trí cláracha teilifíse comhshaoil agus pacáistí acmhainne do bhunscoileanna agus do mheánscoileanna).

BAINISTÍOCHT DRAMHAÍOLA FHORGHNÍOMHACH

- Cur chun cinn seachaint agus laghdú dramhaíola trí chomhordú An Chláir Náisiúnta um Chosc Dramhaíola, lena n-áirítear cur i bhfeidhm na dTionscnamh Freagrachta Táirgeoirí.
- Cur i bhfeidhm Rialachán ar nós na treoracha maidir le Trealamh Leictreach agus Leictreonach Caite agus le Srianadh Substaintí Guaiseacha agus substaintí a dhéanann ídiú ar an gcrios ózóin.
- Plean Náisiúnta Bainistíochta um Dramhaíl Ghuaiseach a fhorbairt chun dramhaíl ghuaiseach a sheachaint agus a bhainistiú.

STRUCHTÚR NA GNÍOMHAIREACHTA

Bunaíodh an Ghníomhaireacht i 1993 chun comhshaol na hÉireann a chosaint. Tá an eagraíocht á bhainistiú ag Bord lánaimseartha, ar a bhfuil Príomhstiúrthóir agus ceithre Stiúrthóir.

Tá obair na Gníomhaireachta ar siúl trí ceithre Oifig:

- An Oifig Aeráide, Ceadúnaithe agus Úsáide Acmhainní
- An Oifig um Fhorfheidhmiúchán Comhshaoil
- An Oifig um Measúnacht Comhshaoil
- An Oifig Cumarsáide agus Seirbhísí Corparáide

Tá Coiste Comhairleach ag an nGníomhaireacht le cabhrú léi. Tá dáréag ball air agus tagann siad le chéile cúpla uair in aghaidh na bliana le plé a dhéanamh ar cheisteanna ar ábhar imní iad agus le comhairle a thabhairt don Bhord.

NDP
National Development Plan 2007 - 2013

Science, Technology, Research and Innovation for the Environment (STRIVE) 2007-2013

The Science, Technology, Research and Innovation for the Environment (STRIVE) programme covers the period 2007 to 2013.

The programme comprises three key measures: Sustainable Development, Cleaner Production and Environmental Technologies, and A Healthy Environment; together with two supporting measures: EPA Environmental Research Centre (ERC) and Capacity & Capability Building. The seven principal thematic areas for the programme are Climate Change; Waste, Resource Management and Chemicals; Water Quality and the Aquatic Environment; Air Quality, Atmospheric Deposition and Noise; Impacts on Biodiversity; Soils and Land-use; and Socio-economic Considerations. In addition, other emerging issues will be addressed as the need arises.

The funding for the programme (approximately €100 million) comes from the Environmental Research Sub-Programme of the National Development Plan (NDP), the Inter-Departmental Committee for the Strategy for Science, Technology and Innovation (IDC-SSTI); and EPA core funding and co-funding by economic sectors.

The EPA has a statutory role to co-ordinate environmental research in Ireland and is organising and administering the STRIVE programme on behalf of the Department of the Environment, Heritage and Local Government.

epa
Environmental Protection Agency
An Ghníomhaireacht um Chaomhnú Comhshaoil

ENVIRONMENTAL PROTECTION AGENCY
PO Box 3000, Johnstown Castle Estate, Co. Wexford, Ireland
t 053 916 0600 f 053 916 0699
LoCall 1890 33 55 99
e info@epa.ie w http://www.epa.ie

SSTI

Comhshaol, Pobal agus Rialtas Áitiúil
Environment, Community and Local Government